NASA TECHNICAL MEMORANDUM

NASA TM X-3463

NASA TECHNICAL MEMORANDUM

NASA TM X-3463

SMALL, LOW-COST, EXPENDABLE TURBOJET ENGINE

II - Performance Characteristics

Robert P. Dengler and Lawrence E. Macioce

Lewis Research Center
Cleveland, Ohio 44135

NATIONAL AERONAUTICS AND SPACE ADMINISTRATION • WASHINGTON, D. C. • DECEMBER 1976

SMALL, LOW-COST, EXPENDABLE TURBOJET ENGINE

II - Performance Characteristics

Robert P. Dengler and Lawrence E. Macioce

Lewis Research Center
Cleveland, Ohio 44135

NATIONAL AERONAUTICS AND SPACE ADMINISTRATION • WASHINGTON, D. C. • DECEMBER 1976

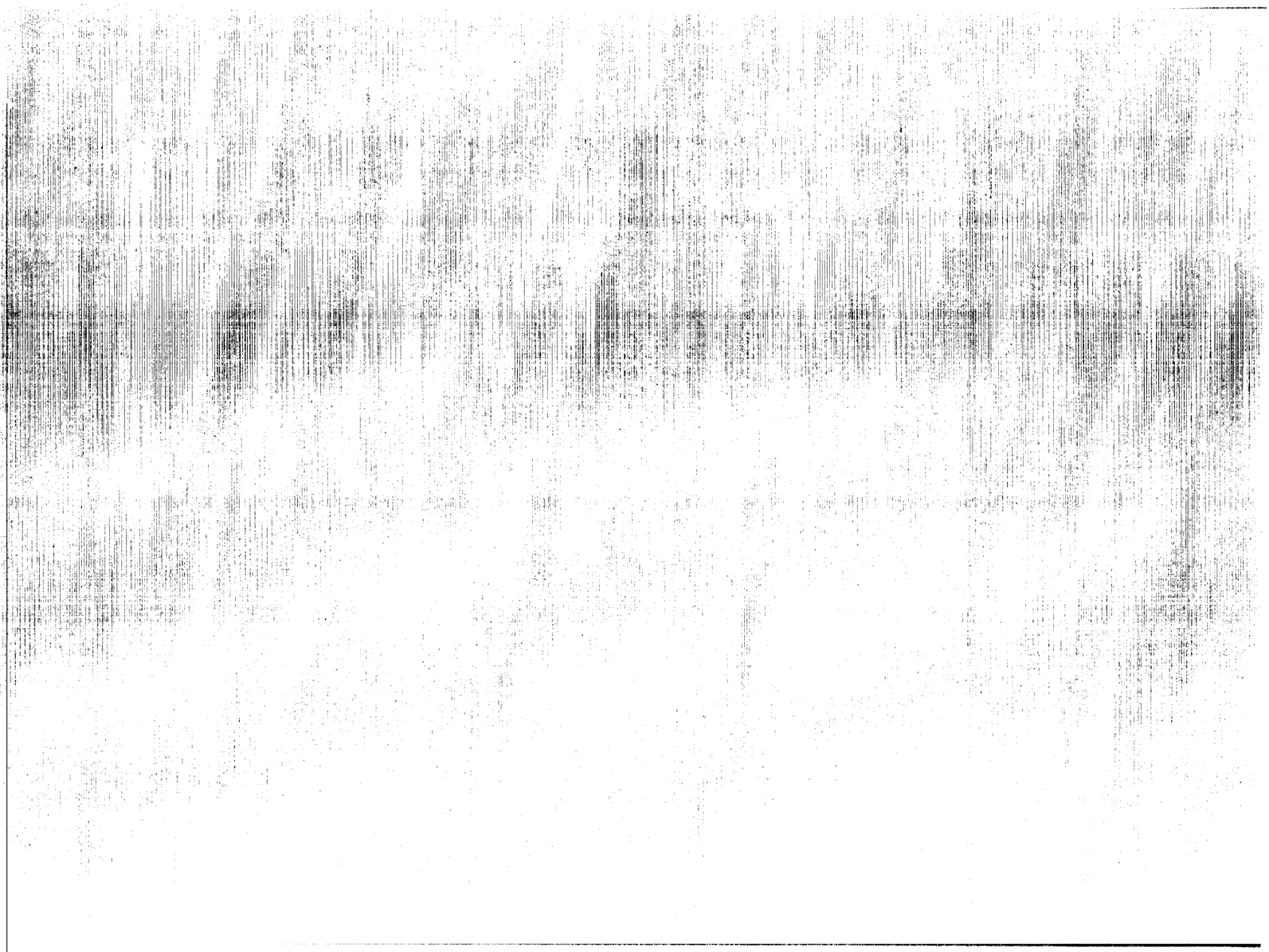

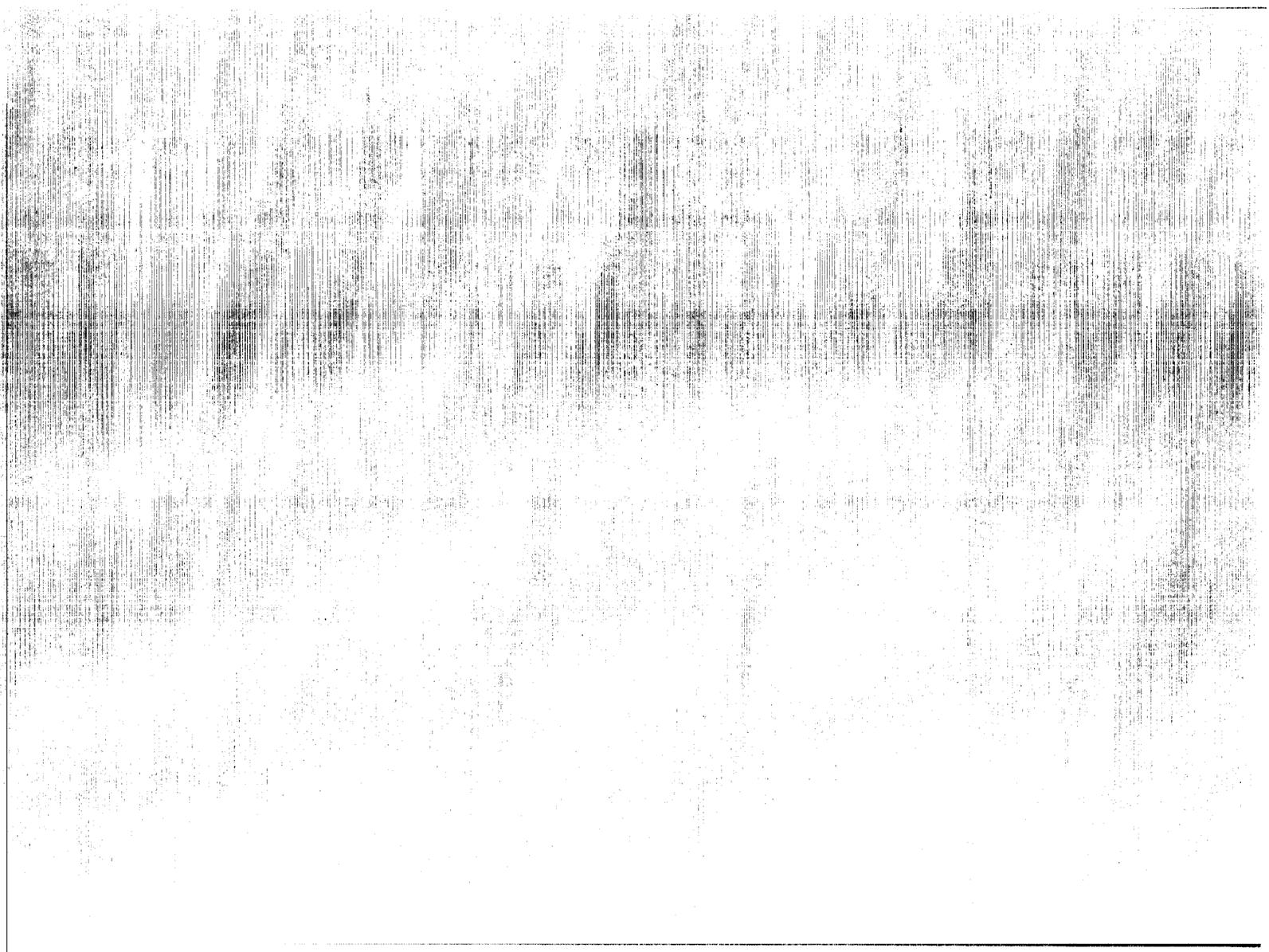

1. Report No.	2. Government Accession No.	3. Recipient's Catalog No.
NASA TM X-3463		

4. Title and Subtitle	5. Report Date
SMALL, LOW-COST, EXPENDABLE TURBOJET ENGINE II - PERFORMANCE CHARACTERISTICS	December 1976
	6. Performing Organization Code
7. Author(s) Robert P. Dengler and Lawrence E. Macioce	8. Performing Organization Report No. E-8775
9. Performing Organization Name and Address Lewis Research Center National Aeronautics and Space Administration Cleveland, Ohio 44135	10. Work Unit No. 505-05
	11. Contract or Grant No.
12. Sponsoring Agency Name and Address National Aeronautics and Space Administration Washington, D.C. 20546	13. Type of Report and Period Covered Technical Memorandum
	14. Sponsoring Agency Code

15. Supplementary Notes

16. Abstract

A small experimental axial-flow turbojet engine was tested at sea level static conditions and over a range of simulated flight conditions to evaluate its performance as well as to demonstrate the feasibility of low-cost concepts utilized in its design. Testing was conducted at engine speeds as high as 37 000 rpm and at turbine inlet temperatures as high as 1272 K (2290° R). For the maximum speed the engine produced a net thrust of 3118 newtons (701 lbf) at sea level static operation and 2318 newtons (520 lbf) at its cruise condition of $M_0 = 0.8$ and 6096 meters (20 000 ft). Data obtained over a range of inlet Reynolds number indexes for nominal M_0 of 0.38 revealed similar effects or trends on compressor characteristics of those previously established for much larger engines.

17. Key Words (Suggested by Author(s))	18. Distribution Statement
Turbojet engines Turbine engines Gas turbine engines	Unclassified - unlimited STAR Category 07

19. Security Classif. (of this report)	20. Security Classif. (of this page)	21. No. of Pages	22. Price*
Unclassified	Unclassified	30	$4.00

* For sale by the National Technical Information Service, Springfield, Virginia 22161

1. Report No.	2. Government Accession No.	3. Recipient's Catalog No.
NASA TM X-3463		

4. Title and Subtitle	5. Report Date
SMALL, LOW-COST, EXPENDABLE TURBOJET ENGINE II - PERFORMANCE CHARACTERISTICS	December 1976
	6. Performing Organization Code
7. Author(s) Robert P. Dengler and Lawrence E. Macioce	8. Performing Organization Report No. E-8775
9. Performing Organization Name and Address Lewis Research Center National Aeronautics and Space Administration Cleveland, Ohio 44135	10. Work Unit No. 505-05
	11. Contract or Grant No.
12. Sponsoring Agency Name and Address National Aeronautics and Space Administration Washington, D.C. 20546	13. Type of Report and Period Covered Technical Memorandum
	14. Sponsoring Agency Code

15. Supplementary Notes

16. Abstract

A small experimental axial-flow turbojet engine was tested at sea level static conditions and over a range of simulated flight conditions to evaluate its performance as well as to demonstrate the feasibility of low-cost concepts utilized in its design. Testing was conducted at engine speeds as high as 37 000 rpm and at turbine inlet temperatures as high as 1272 K (2290° R). For the maximum speed the engine produced a net thrust of 3118 newtons (701 lbf) at sea level static operation and 2318 newtons (520 lbf) at its cruise condition of $M_0 = 0.8$ and 6096 meters (20 000 ft). Data obtained over a range of inlet Reynolds number indexes for nominal M_0 of 0.38 revealed similar effects or trends on compressor characteristics of those previously established for much larger engines.

17. Key Words (Suggested by Author(s))	18. Distribution Statement
Turbojet engines Turbine engines Gas turbine engines	Unclassified - unlimited STAR Category 07

19. Security Classif. (of this report)	20. Security Classif. (of this page)	21. No. of Pages	22. Price*
Unclassified	Unclassified	30	$4.00

* For sale by the National Technical Information Service, Springfield, Virginia 22161

SMALL, LOW-COST, EXPENDABLE TURBOJET ENGINE
II - PERFORMANCE CHARACTERISTICS

by Robert P. Dengler and Lawrence E. Macioce
Lewis Research Center

SUMMARY

A small experimental turbojet engine was tested at sea level static conditions and over a range of simulated flight conditions to demonstrate the feasibility of low cost concepts utilized in its design and to evaluate its performance potential. The basic design was that of an axial-flow turbojet engine with a four-stage compressor, an annular combustor, a single-stage turbine, and a fixed-area exhaust nozzle. The engine had a maximum diameter of 29 centimeters (11.5 in.), an overall length of 96.5 centimeters (38 in.), and weighed about 59 kilograms (130 lb).

Testing was conducted at engine speeds as high as 37 000 rpm and at turbine inlet temperatures as high as 1272 K (2290^{O} R). During sea level static tests, steady-state operation at maximum engine speed resulted in a compressor pressure ratio of about 4.3, an airflow of about 4.9 kilograms per second (10.8 lbm/sec), and a net thrust of 3118 newtons (701 lbf). The engine was subjected to a series of transient tests at sea level to determine its acceleration-deceleration capabilities. In addition, the engine was subjected to continuous operation at maximum test conditions for 1 hour to demonstrate its endurance for short duration missions of expendable applications.

Simulated flight testing was conducted over a range of Mach numbers from 0.18 to 1.24 and altitudes from 610 to 9144 meters (2000 to 30 000 ft). For the design cruise conditions of M_0 = 0.8 and 6096 meters (20 000 ft), operation at the maximum engine speed tested resulted in a compressor pressure ratio of about 4.3, a compressor airflow of about 5 kilograms per second (11 lbm/sec), and a net thrust of 2318 newtons (520 lbf). Data obtained over a range of inlet Reynolds number indexes for a nominal flight Mach number of 0.38 indicated similar effects and trends on compressor characteristics as those previously established for much larger engines.

SMALL, LOW-COST, EXPENDABLE TURBOJET ENGINE
II - PERFORMANCE CHARACTERISTICS
by Robert P. Dengler and Lawrence E. Macioce
Lewis Research Center

SUMMARY

A small experimental turbojet engine was tested at sea level static conditions and over a range of simulated flight conditions to demonstrate the feasibility of low cost concepts utilized in its design and to evaluate its performance potential. The basic design was that of an axial-flow turbojet engine with a four-stage compressor, an annular combustor, a single-stage turbine, and a fixed-area exhaust nozzle. The engine had a maximum diameter of 29 centimeters (11.5 in.), an overall length of 96.5 centimeters (38 in.), and weighed about 59 kilograms (130 lb).

Testing was conducted at engine speeds as high as 37 000 rpm and at turbine inlet temperatures as high as 1272 K (2290^{O} R). During sea level static tests, steady-state operation at maximum engine speed resulted in a compressor pressure ratio of about 4.3, an airflow of about 4.9 kilograms per second (10.8 lbm/sec), and a net thrust of 3118 newtons (701 lbf). The engine was subjected to a series of transient tests at sea level to determine its acceleration-deceleration capabilities. In addition, the engine was subjected to continuous operation at maximum test conditions for 1 hour to demonstrate its endurance for short duration missions of expendable applications.

Simulated flight testing was conducted over a range of Mach numbers from 0.18 to 1.24 and altitudes from 610 to 9144 meters (2000 to 30 000 ft). For the design cruise conditions of M_0 = 0.8 and 6096 meters (20 000 ft), operation at the maximum engine speed tested resulted in a compressor pressure ratio of about 4.3, a compressor airflow of about 5 kilograms per second (11 lbm/sec), and a net thrust of 2318 newtons (520 lbf). Data obtained over a range of inlet Reynolds number indexes for a nominal flight Mach number of 0.38 indicated similar effects and trends on compressor characteristics as those previously established for much larger engines.

INTRODUCTION

This report presents the performance characteristics of a small, low pressure ratio, experimental turbojet engine designed for an expendable-type application. The primary intent of this engine program was to demonstrate some low-cost concepts under study at the NASA Lewis Research Center.

As a means of investigating and demonstrating the feasibility of the basic concepts, the Lewis Research Center and the Naval Weapons Center entered into a joint program for sharing the costs of designing and fabricating a small turbojet engine incorporating a number of the low-cost features. The Navy's primary objective was to demonstrate the feasibility of replacing a rocket engine of a missile with a small, low-cost turbojet engine. Such a substitution appeared particularly attractive since it was expected to improve the payload and range capability as well as result in a significant cost savings. While the concepts employed were aimed primarily at applications utilizing expendable engines, such as drones or remote piloted vehicles (RPV's), in some cases they would apply to light subsonic aircraft as well. References 1 to 5 report on some of the low cost concepts that have been proposed.

Subsequent to analytical studies of candidate engines (refs. 6 to 8), a NASA-Lewis contract was awarded to an engine manufacturer to provide the additional necessary design information along with the final engineering drawings for fabrication purposes. Reference 9 presents the design concepts employed along with some fabricational and preliminary testing aspects. Initial testing was conducted to optimize the overall engine operational characteristics. Such particulars as turbine stator throat area and the camber and setting angles of compressor blades and vanes were adjusted or corrected as required, and the sizing of the fixed area exhaust nozzle was established. A discussion of these developmental-type procedures is included in references 9 and 10.

This report presents the results of performance tests conducted in both sea level static and altitude test stands. Tests were conducted over a range of simulated altitudes from sea level to 9144 meters (30 000 ft), engine speeds from about 26 000 to 37 000 revolutions per minute, average turbine inlet temperatures up to 1272 K (2290° R), and simulated flight Mach numbers up to 1.24. In general, the data are presented for various engine performance parameters plotted as functions of engine speed for the test conditions indicated. In addition, the effects of inlet Reynolds number on selected compressor parameters are presented for a nominal flight Mach number of 0.38.

SYMBOLS

F_n net thrust, N (lbf)

M_0 flight Mach number

INTRODUCTION

This report presents the performance characteristics of a small, low pressure ratio, experimental turbojet engine designed for an expendable-type application. The primary intent of this engine program was to demonstrate some low-cost concepts under study at the NASA Lewis Research Center.

As a means of investigating and demonstrating the feasibility of the basic concepts, the Lewis Research Center and the Naval Weapons Center entered into a joint program for sharing the costs of designing and fabricating a small turbojet engine incorporating a number of the low-cost features. The Navy's primary objective was to demonstrate the feasibility of replacing a rocket engine of a missile with a small, low-cost turbojet engine. Such a substitution appeared particularly attractive since it was expected to improve the payload and range capability as well as result in a significant cost savings. While the concepts employed were aimed primarily at applications utilizing expendable engines, such as drones or remote piloted vehicles (RPV's), in some cases they would apply to light subsonic aircraft as well. References 1 to 5 report on some of the low cost concepts that have been proposed.

Subsequent to analytical studies of candidate engines (refs. 6 to 8), a NASA-Lewis contract was awarded to an engine manufacturer to provide the additional necessary design information along with the final engineering drawings for fabrication purposes. Reference 9 presents the design concepts employed along with some fabricational and preliminary testing aspects. Initial testing was conducted to optimize the overall engine operational characteristics. Such particulars as turbine stator throat area and the camber and setting angles of compressor blades and vanes were adjusted or corrected as required, and the sizing of the fixed area exhaust nozzle was established. A discussion of these developmental-type procedures is included in references 9 and 10.

This report presents the results of performance tests conducted in both sea level static and altitude test stands. Tests were conducted over a range of simulated altitudes from sea level to 9144 meters (30 000 ft), engine speeds from about 26 000 to 37 000 revolutions per minute, average turbine inlet temperatures up to 1272 K (2290° R), and simulated flight Mach numbers up to 1.24. In general, the data are presented for various engine performance parameters plotted as functions of engine speed for the test conditions indicated. In addition, the effects of inlet Reynolds number on selected compressor parameters are presented for a nominal flight Mach number of 0.38.

SYMBOLS

F_n net thrust, N (lbf)

M_0 flight Mach number

N	engine speed, rpm
P	pressure, N/m^2 (psi)
Rel	Reynolds number index, $\delta/\varphi\sqrt{\theta}$
T	temperature, K (^{o}R)
W_a	airflow, kg/sec (lbm/sec)
W_f	fuel flow, kg/hr (lbm/hr)
δ	ratio of total pressure to NACA standard sea-level pressure of 10 129 N/m^2 (14.696 psi)
η_c	compressor efficiency
θ	ratio of total temperature to NACA standard sea-level temperature of 288.1 K (518.7^{o} R)
φ	ratio of coefficient of viscosity corresponding with total temperature to coefficient of viscosity corresponding with NACA standard sea-level temperature of 288.1 K (518.7^{o} R)

Subscripts:

R	rated
s	static
t	total
1 to 6	engine stations

APPARATUS

Engine Design and Description

The expendable-type engine design generated for this investigation was that of an axial-flow turbojet engine with a four-stage compressor, an annular combustor, a single-stage turbine, and a fixed area exhaust nozzle. The basic requirements of the engine were that it be small and relatively lightweight. In addition, the engine should be capable of an air launch start, produce a thrust of 2674 newtons (600 lbf) at sea level static conditions and 1560 newtons (350 lbf) at its cruise condition, and be self-sufficient for a 20-minute mission. More specifically, the engine was designed to satisfy the operating characteristics, internal gas conditions, and other requirements summarized in table I.

The cross-sectional view of the engine design presented in figure 1 shows the engine to have a maximum diameter of 29.2 centimeters (11.5 in.) and a length of 96.5 centi-

N	engine speed, rpm
P	pressure, N/m^2 (psi)
Rel	Reynolds number index, $\delta/\varphi\sqrt{\theta}$
T	temperature, K (^{o}R)
W_a	airflow, kg/sec (lbm/sec)
W_f	fuel flow, kg/hr (lbm/hr)
δ	ratio of total pressure to NACA standard sea-level pressure of 10 129 N/m^2 (14.696 psi)
η_c	compressor efficiency
θ	ratio of total temperature to NACA standard sea-level temperature of 288.1 K (518.7^{o} R)
φ	ratio of coefficient of viscosity corresponding with total temperature to coefficient of viscosity corresponding with NACA standard sea-level temperature of 288.1 K (518.7^{o} R)

Subscripts:

R	rated
s	static
t	total
1 to 6	engine stations

APPARATUS

Engine Design and Description

The expendable-type engine design generated for this investigation was that of an axial-flow turbojet engine with a four-stage compressor, an annular combustor, a single-stage turbine, and a fixed area exhaust nozzle. The basic requirements of the engine were that it be small and relatively lightweight. In addition, the engine should be capable of an air launch start, produce a thrust of 2674 newtons (600 lbf) at sea level static conditions and 1560 newtons (350 lbf) at its cruise condition, and be self-sufficient for a 20-minute mission. More specifically, the engine was designed to satisfy the operating characteristics, internal gas conditions, and other requirements summarized in table I.

The cross-sectional view of the engine design presented in figure 1 shows the engine to have a maximum diameter of 29.2 centimeters (11.5 in.) and a length of 96.5 centi-

3

meters (38 in.). The basic weight of the engine was 59 kilograms (130 lbm). Figure 2, by showing the major components of this engine surrounding an assembled version, illustrates the simplicity of this design.

A number of low-cost features were incorporated in this engine design and are discussed in reference 9. A detailed description of the engine components and some of the fabrication and assembly aspects are also included in this reference.

Test Facilities

Two separate facilities were used to conduct the test programs for this experimental engine. All sea level static testing was conducted in the Special Projects Laboratory (SPL) of the NASA Lewis Research Center. Figure 3(a) shows the engine installed in SPL. All the simulated flight testing for this engine was conducted in the Propulsion Systems Laboratory (PSL), and figure 3(b) shows the engine installed in this facility. In lieu of the integral-type bellmouth inlet used in the sea level static tests, a conventional direct connect arrangement employing a labyrinth slip seal was used to allow insertion of the inlet section into the plenum chamber where ram air conditions were provided for engine operation.

Instrumentation

Research and operational instrumentation were provided on the engine in order to determine the engine performance characteristics and to ensure safe operating conditions. Figure 4 is a schematic of the engine showing the respective locations of various engine stations where pressure and/or temperature measurements were made to determine flow conditions of the gas stream. All temperature measurements were made with Chromel-Alumel-type thermocouples, while static pressures were obtained from wall taps and total pressures from probes or rakes inserted into the air or gas stream. Other important measurements included bearing temperatures, engine speed, fuel flow, engine thrust, and engine vibrations. Two accelerometers located at the front and the rear of the engine were positioned to indicate the vibration levels in both the vertical and horizontal direction. A proximity probe was mounted directly over a retaining ring which housed the outer race of the front bearing in order to provide an indication of the shaft displacement. Most measurements were recorded on the Central Automatic Digital Data Encoder (CADDE) system. Temperatures, fuel flows, engine speed, etc., were recorded as voltage outputs through the Automatic Voltage Digitizer (AVD) system, and pressures were obtained through the use of scanivalve transducers or the Digital Automatic Multiple

meters (38 in.). The basic weight of the engine was 59 kilograms (130 lbm). Figure 2, by showing the major components of this engine surrounding an assembled version, illustrates the simplicity of this design.

A number of low-cost features were incorporated in this engine design and are discussed in reference 9. A detailed description of the engine components and some of the fabrication and assembly aspects are also included in this reference.

Test Facilities

Two separate facilities were used to conduct the test programs for this experimental engine. All sea level static testing was conducted in the Special Projects Laboratory (SPL) of the NASA Lewis Research Center. Figure 3(a) shows the engine installed in SPL. All the simulated flight testing for this engine was conducted in the Propulsion Systems Laboratory (PSL), and figure 3(b) shows the engine installed in this facility. In lieu of the integral-type bellmouth inlet used in the sea level static tests, a conventional direct connect arrangement employing a labyrinth slip seal was used to allow insertion of the inlet section into the plenum chamber where ram air conditions were provided for engine operation.

Instrumentation

Research and operational instrumentation were provided on the engine in order to determine the engine performance characteristics and to ensure safe operating conditions. Figure 4 is a schematic of the engine showing the respective locations of various engine stations where pressure and/or temperature measurements were made to determine flow conditions of the gas stream. All temperature measurements were made with Chromel-Alumel-type thermocouples, while static pressures were obtained from wall taps and total pressures from probes or rakes inserted into the air or gas stream. Other important measurements included bearing temperatures, engine speed, fuel flow, engine thrust, and engine vibrations. Two accelerometers located at the front and the rear of the engine were positioned to indicate the vibration levels in both the vertical and horizontal direction. A proximity probe was mounted directly over a retaining ring which housed the outer race of the front bearing in order to provide an indication of the shaft displacement. Most measurements were recorded on the Central Automatic Digital Data Encoder (CADDE) system. Temperatures, fuel flows, engine speed, etc., were recorded as voltage outputs through the Automatic Voltage Digitizer (AVD) system, and pressures were obtained through the use of scanivalve transducers or the Digital Automatic Multiple

Pressure Recording (DAMPR) system. The data were then processed in a digital computer. A detailed description of the CADDE system is given in reference 11. A number of duplicate measurements were also recorded on roll strip charts in order to provide a continuous record of selected parameters during the tests. The calibration accuracy of the instruments used to obtain measurements during this investigation are listed as percent error:

	Percent error
Scanivalve	0.1
DAMPR	.1
Load cell	.1
Digital counter	.1
Thermocouple	.4
Flowmeter	.5

Test Procedures

As indicated in reference 9, the camber and/or setting angles of the compressor blading were adjusted in preliminary testing, and the optimum sizing of the turbine stator throat area and the exhaust nozzle were established. No departure from this established engine geometry was made in any of the testing reported herein. The engine utilized an exhaust nozzle having a discharge area of 94 square centimeters (37 sq in.), and it was equipped with the simplified fuel control referred to in reference 9.

At sea level static conditions the normal procedure for obtaining steady-state data was to operate the engine over a range of speeds from about 74 to 107 percent of the design rated corrected speed of 35 170 revolutions per minute. Data were recorded through the automatic CADDE data recording system at engine speed increments of approximately 5 to 10 percent.

Following this mode of testing the acceleration-deceleration characteristics of the engine were evaluated to determine the engine's transient response with particular attention directed toward compressor surge or combustor flameout problems. Subsequent to the previous testing, and with engine still installed in the SPL facility, the engine was subjected to an endurance-type test at conditions more severe than the original sea level design point.

With the engine installed in the altitude chamber of the PSL facility, a series of tests was conducted over a range of simulated flight conditions within a proposed operating

Pressure Recording (DAMPR) system. The data were then processed in a digital computer. A detailed description of the CADDE system is given in reference 11. A number of duplicate measurements were also recorded on roll strip charts in order to provide a continuous record of selected parameters during the tests. The calibration accuracy of the instruments used to obtain measurements during this investigation are listed as percent error:

	Percent error
Scanivalve	0.1
DAMPR	.1
Load cell	.1
Digital counter	.1
Thermocouple	.4
Flowmeter	.5

Test Procedures

As indicated in reference 9, the camber and/or setting angles of the compressor blading were adjusted in preliminary testing, and the optimum sizing of the turbine stator throat area and the exhaust nozzle were established. No departure from this established engine geometry was made in any of the testing reported herein. The engine utilized an exhaust nozzle having a discharge area of 94 square centimeters (37 sq in.), and it was equipped with the simplified fuel control referred to in reference 9.

At sea level static conditions the normal procedure for obtaining steady-state data was to operate the engine over a range of speeds from about 74 to 107 percent of the design rated corrected speed of 35 170 revolutions per minute. Data were recorded through the automatic CADDE data recording system at engine speed increments of approximately 5 to 10 percent.

Following this mode of testing the acceleration-deceleration characteristics of the engine were evaluated to determine the engine's transient response with particular attention directed toward compressor surge or combustor flameout problems. Subsequent to the previous testing, and with engine still installed in the SPL facility, the engine was subjected to an endurance-type test at conditions more severe than the original sea level design point.

With the engine installed in the altitude chamber of the PSL facility, a series of tests was conducted over a range of simulated flight conditions within a proposed operating

envelope. These altitude tests followed much the same testing procedure as that used for the steady-state sea level static tests. Only limited transient (acceleration-deceleration) tests were conducted at altitude conditions.

At simulated flight conditions the ram air supplied to the engine inlet was used to windmill the engine to adequate speeds in accommodating an engine start. Different windmilling speeds generally necessitated adjusting the fuel control to obtain the required fuel flow rate for proper engine starting.

Although temperature measurements were not obtained at the turbine inlet (station 4), temperatures were calculated for this station using measured temperatures at station 6. For a jet exhaust temperature of 1144 K (2060° R) the turbine inlet temperature was calculated to be about 1272 K (2290° R) at sea level static conditions.

RESULTS AND DISCUSSION

Engine testing was conducted at both sea level static and simulated flight conditions. Engine speeds as high as 37 000 rpm and turbine inlet temperatures as high as 1272 K (2290° R) were investigated at sea level static conditions. Testing at simulated flight conditions included Mach numbers from 0.18 to 1.24 and altitudes from 610 to 9144 meters (2000 to 30 000 ft).

The following paragraphs discuss the results of tests conducted on the engine for determining its performance characteristics. The results are presented in the following order:

- Sea level static operation:
  - Steady-state characteristics
  - Transient characteristics
  - Endurance testing
- Simulated flight operation:
  - Windmill engine starts
  - Steady-state characteristics
  - Reynolds number index correlation

Sea Level Static Operation

Steady-state characteristics. - Data for steady-state operation at sea level static conditions were obtained over a range of corrected engine speeds from about 74 to 107 percent of the rated design value of 35 170 rpm. Where applicable the data used for the

envelope. These altitude tests followed much the same testing procedure as that used for the steady-state sea level static tests. Only limited transient (acceleration-deceleration) tests were conducted at altitude conditions.

At simulated flight conditions the ram air supplied to the engine inlet was used to windmill the engine to adequate speeds in accommodating an engine start. Different windmilling speeds generally necessitated adjusting the fuel control to obtain the required fuel flow rate for proper engine starting.

Although temperature measurements were not obtained at the turbine inlet (station 4), temperatures were calculated for this station using measured temperatures at station 6. For a jet exhaust temperature of 1144 K (2060° R) the turbine inlet temperature was calculated to be about 1272 K (2290° R) at sea level static conditions.

RESULTS AND DISCUSSION

Engine testing was conducted at both sea level static and simulated flight conditions. Engine speeds as high as 37 000 rpm and turbine inlet temperatures as high as 1272 K (2290° R) were investigated at sea level static conditions. Testing at simulated flight conditions included Mach numbers from 0.18 to 1.24 and altitudes from 610 to 9144 meters (2000 to 30 000 ft).

The following paragraphs discuss the results of tests conducted on the engine for determining its performance characteristics. The results are presented in the following order:

- Sea level static operation:
  - Steady-state characteristics
  - Transient characteristics
  - Endurance testing
- Simulated flight operation:
  - Windmill engine starts
  - Steady-state characteristics
  - Reynolds number index correlation

Sea Level Static Operation

Steady-state characteristics. - Data for steady-state operation at sea level static conditions were obtained over a range of corrected engine speeds from about 74 to 107 percent of the rated design value of 35 170 rpm. Where applicable the data used for the

figures in this report have been normalized to standard pressure and temperature conditions at sea level.

Figure 5 presents data plotted to reveal performance characteristics of the engine's compressor. Parameters of pressure ratio, temperature ratio, corrected airflow, and efficiency are presented in figures 5(a) to (d) as functions of the percent of rated corrected engine speed, and figure 5(e) presents the compressor pressure ratio as a function of the compressor's corrected airflow. The curve resulting from the plotted data in figure 5(e) represents the normal engine operating line for these sea level static conditions.

The engine performance characteristics are presented in figures 6(a) to (f) by plotting the parameters of corrected jet exhaust temperature, engine pressure ratio, engine temperature ratio, corrected net thrust, corrected fuel flow, and specific fuel consumption as functions of the percent of rated corrected engine speed. Table II presents a comparison of design values for selected performance parameters with corresponding test data for operation at the rated corrected engine speed condition of 35 170 rpm. The design values listed are derived from table I and have been normalized to standard sea level conditions. The values for actual test data were obtained from the curves of figures 5(a) to (d) and 6(a) to (e). In addition, this table also presents similar information for actual engine operation at the maximum test condition of 107 percent of rated corrected engine speed. Operation at this maximum condition resulted in a compressor pressure ratio of 4.32, a corrected compressor airflow of 4.89 kilograms per second (10.79 lb/sec), and a net thrust of 3118 newtons (701 lbf).

A significant difference exists between the design and operational values of compressor efficiency at the rated engine speed condition. The design value for compressor efficiency was 0.83, whereas the actual experimental value was only 0.74. As shown in figure 5(d), the test results revealed a rather low compressor efficiency over the entire range of speeds investigated. From an engine speed of about 75 percent of the rated corrected value the compressor efficiency increases from about 0.689 to a peak of 0.745 at 96 percent of rated speed and then drops off significantly at higher speeds. As discussed in reference 9, some adjustments to the compressor blading were made in the preliminary testing without much success in improving compressor efficiency; the conclusion being that it would take a major redesign effort to increase the compressor efficiency to the desired design values. This poor efficiency is reflected in the discrepancies noted between the design and operational values (at rated speed) of weight flow and pressure and temperature ratios of the compressor. The overall engine pressure ratio is lower than the respective design value by about 17 percent. The required fuel flow is somewhat lower than that of the design value, but then the airflow is also somewhat lower. Actually, the fuel/air ratio for both design and actual operation at this rated speed condition is approximately the same at 0.018. In the category of net thrust, the test data show a value that was approximately 14 percent lower than that of design. This

figures in this report have been normalized to standard pressure and temperature conditions at sea level.

Figure 5 presents data plotted to reveal performance characteristics of the engine's compressor. Parameters of pressure ratio, temperature ratio, corrected airflow, and efficiency are presented in figures 5(a) to (d) as functions of the percent of rated corrected engine speed, and figure 5(e) presents the compressor pressure ratio as a function of the compressor's corrected airflow. The curve resulting from the plotted data in figure 5(e) represents the normal engine operating line for these sea level static conditions.

The engine performance characteristics are presented in figures 6(a) to (f) by plotting the parameters of corrected jet exhaust temperature, engine pressure ratio, engine temperature ratio, corrected net thrust, corrected fuel flow, and specific fuel consumption as functions of the percent of rated corrected engine speed. Table II presents a comparison of design values for selected performance parameters with corresponding test data for operation at the rated corrected engine speed condition of 35 170 rpm. The design values listed are derived from table I and have been normalized to standard sea level conditions. The values for actual test data were obtained from the curves of figures 5(a) to (d) and 6(a) to (e). In addition, this table also presents similar information for actual engine operation at the maximum test condition of 107 percent of rated corrected engine speed. Operation at this maximum condition resulted in a compressor pressure ratio of 4.32, a corrected compressor airflow of 4.89 kilograms per second (10.79 lb/sec), and a net thrust of 3118 newtons (701 lbf).

A significant difference exists between the design and operational values of compressor efficiency at the rated engine speed condition. The design value for compressor efficiency was 0.83, whereas the actual experimental value was only 0.74. As shown in figure 5(d), the test results revealed a rather low compressor efficiency over the entire range of speeds investigated. From an engine speed of about 75 percent of the rated corrected value the compressor efficiency increases from about 0.689 to a peak of 0.745 at 96 percent of rated speed and then drops off significantly at higher speeds. As discussed in reference 9, some adjustments to the compressor blading were made in the preliminary testing without much success in improving compressor efficiency; the conclusion being that it would take a major redesign effort to increase the compressor efficiency to the desired design values. This poor efficiency is reflected in the discrepancies noted between the design and operational values (at rated speed) of weight flow and pressure and temperature ratios of the compressor. The overall engine pressure ratio is lower than the respective design value by about 17 percent. The required fuel flow is somewhat lower than that of the design value, but then the airflow is also somewhat lower. Actually, the fuel/air ratio for both design and actual operation at this rated speed condition is approximately the same at 0.018. In the category of net thrust, the test data show a value that was approximately 14 percent lower than that of design. This

deficiency reflects itself in the specific fuel consumption which results in a value about 15 percent higher than the design value. When the engine speed was increased to the maximum speed of 37 000 rpm ($N/\sqrt{\theta_2}$ = 107 percent of rated) the compressor efficiency dropped to about 0.702. Despite this low efficiency, the engine operation resulted in a net thrust of 3118 newtons (701 lbf) at this overspeed condition. This resultant thrust is 445 newtons (100 lbf) greater than the required design value at rated speed. For these test conditions, the actual mechanical speed (N) of 37 000 rpm represented a 5-percent increase over that of the design value of 35 170 rpm. However, when the engine speed was corrected to standard sea level conditions the parameter $N/\sqrt{\theta_2}$ resulted in 107 percent of the design rated corrected engine speed.

Transient characteristics. - The engine was subjected to a series of transient tests in which the engine was accelerated from a moderate speed of about 26 000 rpm (75 percent of the rated speed) to a predetermined higher speed; after the engine was stabilized, it was decelerated to the initial speed. Throttle transients of this nature were made to peak engine speeds of about 85, 95, and 105 percent of the corrected rated engine speed. The engine accelerations and decelerations were accomplished by a smooth, continuous movement of the throttle (manually) for increments of about 5, 3, and less than 1/2 second (snap acceleration).

Generally speaking, the speed excursions for the slower throttle movements were easily accomplished, but the snap accelerations generally caused compressor surge during early tests. From preliminary testing of this engine (ref. 9) it was already evident that the operating line for steady-state operating conditions for sea level static testing was close to the compressor surge line. Despite this, and following some modifications to the fuel control, the engine did complete all of the prescribed snap accelerations and decelerations without experiencing a surge condition in subsequent testing. In addition, no problems were experienced with regard to combustor flameout during any of the transient testing. Figure 7 shows data plotted from charts of continuous recordings for a snap acceleration from about 75 to 105 percent of rated engine speed, and a subsequent snap deceleration back to the initial speed. The engine throttle position and the engine speed are plotted in figures 7(a) and (b), respectively, as functions of elapsed time in seconds. The time required for the engine to accelerate to the preset condition of 105 percent of rated engine speed was just under 6 seconds. The engine was allowed to stabilize at this speed for a period of seconds - up to a minute or so - before a snap deceleration was performed. Once again, the fuel control quickly responded to the rapid throttle movement and the engine speed was reduced to about 75 percent speed in under 4 seconds.

The performance of the fuel control for this speed excursion is illustrated in figure 8. A generalized parameter consisting of corrected fuel flow $\left(W_f/\delta_2\sqrt{\theta_2}\right)$ divided by percent of rated corrected engine speed $\left(\%N_R/\sqrt{\theta_2}\right)$ is plotted against the compressor

deficiency reflects itself in the specific fuel consumption which results in a value about 15 percent higher than the design value. When the engine speed was increased to the maximum speed of 37 000 rpm ($N/\sqrt{\theta_2}$ = 107 percent of rated) the compressor efficiency dropped to about 0.702. Despite this low efficiency, the engine operation resulted in a net thrust of 3118 newtons (701 lbf) at this overspeed condition. This resultant thrust is 445 newtons (100 lbf) greater than the required design value at rated speed. For these test conditions, the actual mechanical speed (N) of 37 000 rpm represented a 5-percent increase over that of the design value of 35 170 rpm. However, when the engine speed was corrected to standard sea level conditions the parameter $N/\sqrt{\theta_2}$ resulted in 107 percent of the design rated corrected engine speed.

Transient characteristics. - The engine was subjected to a series of transient tests in which the engine was accelerated from a moderate speed of about 26 000 rpm (75 percent of the rated speed) to a predetermined higher speed; after the engine was stabilized, it was decelerated to the initial speed. Throttle transients of this nature were made to peak engine speeds of about 85, 95, and 105 percent of the corrected rated engine speed. The engine accelerations and decelerations were accomplished by a smooth, continuous movement of the throttle (manually) for increments of about 5, 3, and less than 1/2 second (snap acceleration).

Generally speaking, the speed excursions for the slower throttle movements were easily accomplished, but the snap accelerations generally caused compressor surge during early tests. From preliminary testing of this engine (ref. 9) it was already evident that the operating line for steady-state operating conditions for sea level static testing was close to the compressor surge line. Despite this, and following some modifications to the fuel control, the engine did complete all of the prescribed snap accelerations and decelerations without experiencing a surge condition in subsequent testing. In addition, no problems were experienced with regard to combustor flameout during any of the transient testing. Figure 7 shows data plotted from charts of continuous recordings for a snap acceleration from about 75 to 105 percent of rated engine speed, and a subsequent snap deceleration back to the initial speed. The engine throttle position and the engine speed are plotted in figures 7(a) and (b), respectively, as functions of elapsed time in seconds. The time required for the engine to accelerate to the preset condition of 105 percent of rated engine speed was just under 6 seconds. The engine was allowed to stabilize at this speed for a period of seconds - up to a minute or so - before a snap deceleration was performed. Once again, the fuel control quickly responded to the rapid throttle movement and the engine speed was reduced to about 75 percent speed in under 4 seconds.

The performance of the fuel control for this speed excursion is illustrated in figure 8. A generalized parameter consisting of corrected fuel flow $\left(W_f/\delta_2\sqrt{\theta_2}\right)$ divided by percent of rated corrected engine speed $\left(\%N_R/\sqrt{\theta_2}\right)$ is plotted against the compressor

pressure ratio ($P_{t,3}/P_{t,2}$). As discussed in reference 3, this fuel control concept is based on the assumption that the maximum and minimum fuel limits can be described by linear functions of corrected engine parameters. As shown in the figure, straight lines have been drawn through data points to depict the acceleration and deceleration limits which can be preset through adjustments on the fuel control mechanism.

Endurance testing. - In order to verify the engine capabilities with respect to the life requirements for the proposed application, an endurance-type test was conducted at the maximum speed condition of 37 000 rpm with the 94 square centimeter (37 $in.^2$) exhaust nozzle for 1 hour of continuous operation. The performance results of this test are presented in table II, and they are also shown in figures 5 and 6 for 107 percent of the rated corrected engine speed. The data presented are for the average of 12 steady-state readings taken during the 1-hour endurance test. The average corrected thrust rating for this endurance test was 3118 newtons (701 lbf), which exceeded the Naval Weapons Center requirement of 2669 newtons (600 lbf) for sea level static operation. Since the duration of the proposed mission for the NWC engine demonstration was of the order of 20 minutes, this endurance test was considered more than adequate.

Simulated Flight Operation

Data for steady-state operation at engine speeds from about 74 to 107 percent of the rated corrected design value were obtained over a range of simulated flight conditions. These operating conditions covered a range of flight Mach numbers from 0.17 to 1.24 and representative altitudes from 610 to 9144 meters (2000 to 30 000 ft). A summary tabulation of operating conditions is presented in table III. Figure 9, which presents the operating conditions listed in table III as a plot of flight Mach number against altitude, illustrates the intended operating envelope. Also shown plotted in this figure are the representative conditions for which successful windmilling engine starts were achieved.

Windmill engine starts. - For an engine to be started in flight from windmilling conditions, it is important to determine the compressor airflow in order to ensure adequate conditions for combustion along with proper adjustments to the fuel control for acceptable fuel flow schedules. The windmilling characteristics for this engine are illustrated in figure 10. This figure presents corrected windmilling speed and corrected compressor weight flow plotted as a function of flight Mach number. Extended windmilling operation was avoided because of unfavorable front-bearing lubrication qualtities at this condition. The oil-mist bearing lubrication deficiency was caused by an adverse pressure gradient that existed between the bearing cavity on one side of the bearing and the compressor rotor inlet region on the other side of the bearing. As a consequence, only a representative number of windmilling conditions were attempted. The curve of figure 10(a) indicates that the corrected windmilling speed is directly proportional to the flight Mach

pressure ratio ($P_{t,3}/P_{t,2}$). As discussed in reference 3, this fuel control concept is based on the assumption that the maximum and minimum fuel limits can be described by linear functions of corrected engine parameters. As shown in the figure, straight lines have been drawn through data points to depict the acceleration and deceleration limits which can be preset through adjustments on the fuel control mechanism.

Endurance testing. - In order to verify the engine capabilities with respect to the life requirements for the proposed application, an endurance-type test was conducted at the maximum speed condition of 37 000 rpm with the 94 square centimeter (37 $in.^2$) exhaust nozzle for 1 hour of continuous operation. The performance results of this test are presented in table II, and they are also shown in figures 5 and 6 for 107 percent of the rated corrected engine speed. The data presented are for the average of 12 steady-state readings taken during the 1-hour endurance test. The average corrected thrust rating for this endurance test was 3118 newtons (701 lbf), which exceeded the Naval Weapons Center requirement of 2669 newtons (600 lbf) for sea level static operation. Since the duration of the proposed mission for the NWC engine demonstration was of the order of 20 minutes, this endurance test was considered more than adequate.

Simulated Flight Operation

Data for steady-state operation at engine speeds from about 74 to 107 percent of the rated corrected design value were obtained over a range of simulated flight conditions. These operating conditions covered a range of flight Mach numbers from 0.17 to 1.24 and representative altitudes from 610 to 9144 meters (2000 to 30 000 ft). A summary tabulation of operating conditions is presented in table III. Figure 9, which presents the operating conditions listed in table III as a plot of flight Mach number against altitude, illustrates the intended operating envelope. Also shown plotted in this figure are the representative conditions for which successful windmilling engine starts were achieved.

Windmill engine starts. - For an engine to be started in flight from windmilling conditions, it is important to determine the compressor airflow in order to ensure adequate conditions for combustion along with proper adjustments to the fuel control for acceptable fuel flow schedules. The windmilling characteristics for this engine are illustrated in figure 10. This figure presents corrected windmilling speed and corrected compressor weight flow plotted as a function of flight Mach number. Extended windmilling operation was avoided because of unfavorable front-bearing lubrication qualtities at this condition. The oil-mist bearing lubrication deficiency was caused by an adverse pressure gradient that existed between the bearing cavity on one side of the bearing and the compressor rotor inlet region on the other side of the bearing. As a consequence, only a representative number of windmilling conditions were attempted. The curve of figure 10(a) indicates that the corrected windmilling speed is directly proportional to the flight Mach

number. The data plotted in figure 10(b) indicate that although the corrected compressor weight flow is not directly proportional to the flight Mach number, it is some function of that parameter. Engine starts from the windmilling condition were made at three different flight Mach number conditions of about 0.38, 0.65, and 0.82 (see fig. 9). At the Mach number of 0.38, engine starts were successfully attempted at altitudes of 1524, 3048, 4572, and 6096 meters (5000, 10 000, 15 000, and 20 000 ft). Once again, in the interest of preserving engine life and reducing testing time, only a minimum number of engine starts were attempted. The conditions for which engine starts were attempted and successfully completed were considered adequate for the intended application.

Steady-state characteristics. - The steady-state performance characteristics of this engine at simulated flight conditions are presented in figures 11 and 12. The format presentation of these data is similar to that for sea level static conditions; also, as a convenience for comparative purposes, the curve for the sea level data is also presented in these figures. For the purpose of clarity, only data for nominal flight Mach numbers of 0.24, 0.50, 0.82, and 1.24 have been selected as being representative to show the trends and characteristics.

The plotted data of figure 11 reveal the compressor performance characteristics for simulated flight conditions. Plots of the compressor parameters, pressure ratio, temperature ratio, and corrected airflow, are presented as functions of percent of rated corrected engine speed in figures 11(a) to (c), respectively. Curves are presented in these figures for only the sea level static condition (M = 0.0) and the maximum flight speed condition of M = 1.24. These two curves form the boundaries for the band of test data plotted. Figure 11(d) presents data for the compressor parameter, pressure ratio, plotted as a function of the compressor corrected airflow. Curves, or operating lines, are presented for data of all the flight Mach number conditions plotted; in addition to the sea level static data curve being presented, the compressor surge line curve for this engine has been replotted from reference 9. As indicated by this figure, the effect of increasing the flight Mach number (increasing ram pressure) is to shift the operating line away from the surge line. At the design cruise Mach number of 0.80 this engine then has ample stall margin with the exhaust nozzle having a discharge area of 94 square centimeters (37 in.^{2}).

Reference 12 presents an analog computer simulation of this basic engine design for determining the performance characteristics for various test conditions. Slight variations in inlet operating conditions, efficiencies, and exhaust nozzle sizing prevented a direct comparison of the engine simulation data with the original design data of table I for either the sea level static or cruise condition. Although the data are not directly comparable, the general trends for the engine operational data presented herein closely resemble the results of the engine simulation study. It will be seen that in both the results of reference 12 and in figures 11 and 12 of this report that the data tend to converge

number. The data plotted in figure 10(b) indicate that although the corrected compressor weight flow is not directly proportional to the flight Mach number, it is some function of that parameter. Engine starts from the windmilling condition were made at three different flight Mach number conditions of about 0.38, 0.65, and 0.82 (see fig. 9). At the Mach number of 0.38, engine starts were successfully attempted at altitudes of 1524, 3048, 4572, and 6096 meters (5000, 10 000, 15 000, and 20 000 ft). Once again, in the interest of preserving engine life and reducing testing time, only a minimum number of engine starts were attempted. The conditions for which engine starts were attempted and successfully completed were considered adequate for the intended application.

Steady-state characteristics. - The steady-state performance characteristics of this engine at simulated flight conditions are presented in figures 11 and 12. The format presentation of these data is similar to that for sea level static conditions; also, as a convenience for comparative purposes, the curve for the sea level data is also presented in these figures. For the purpose of clarity, only data for nominal flight Mach numbers of 0.24, 0.50, 0.82, and 1.24 have been selected as being representative to show the trends and characteristics.

The plotted data of figure 11 reveal the compressor performance characteristics for simulated flight conditions. Plots of the compressor parameters, pressure ratio, temperature ratio, and corrected airflow, are presented as functions of percent of rated corrected engine speed in figures 11(a) to (c), respectively. Curves are presented in these figures for only the sea level static condition (M = 0.0) and the maximum flight speed condition of M = 1.24. These two curves form the boundaries for the band of test data plotted. Figure 11(d) presents data for the compressor parameter, pressure ratio, plotted as a function of the compressor corrected airflow. Curves, or operating lines, are presented for data of all the flight Mach number conditions plotted; in addition to the sea level static data curve being presented, the compressor surge line curve for this engine has been replotted from reference 9. As indicated by this figure, the effect of increasing the flight Mach number (increasing ram pressure) is to shift the operating line away from the surge line. At the design cruise Mach number of 0.80 this engine then has ample stall margin with the exhaust nozzle having a discharge area of 94 square centimeters (37 in.^{2}).

Reference 12 presents an analog computer simulation of this basic engine design for determining the performance characteristics for various test conditions. Slight variations in inlet operating conditions, efficiencies, and exhaust nozzle sizing prevented a direct comparison of the engine simulation data with the original design data of table I for either the sea level static or cruise condition. Although the data are not directly comparable, the general trends for the engine operational data presented herein closely resemble the results of the engine simulation study. It will be seen that in both the results of reference 12 and in figures 11 and 12 of this report that the data tend to converge

at the higher engine speeds for all Mach number conditions. For a condition of increased Mach number the engine tends to operate at lower jet exhaust (and therefore lower turbine inlet and outlet) gas temperatures (see fig. 12(a)), which results in contributing to the lower net thrust values (see fig. 12(d)). At the design cruise condition (M_0 = 0.8, 6096 m (20 000 ft)) experimental data indicated that the engine was operating at a corrected jet exhaust temperature of 808 K (1455° R) with a corrected net thrust of 1382 newtons (310 lbf) compared to 1007 K (1812° R) and 1640 newtons (368 lbf) for the corrected design values of table I. At the maximum mechanical speed of 37 000 rpm (corrected rated engine speed of 107 percent), however, the engine operated with a corrected jet exhaust temperature of 1036 K (1865° R) resulting in a corrected net thrust of 2318 newtons (520 lbf). For these maximum test conditions the thrust value was in excess of the Naval Weapons Center's cruise condition requirement by more than 669 newtons (150 lbf).

Reynolds number index correlation. - The basic objective of this investigation, with regard to engine operation, was to obtain data for sea level static conditions and for a range of simulated flight conditions within the operational envelope of figure 9 in order to allow the Naval Weapons Center to integrate this information into their demonstration test plans. The performance characteristics of this engine have been presented thus far without regard for effects on performance due to variation inlet Reynolds number index $\left(\delta_2/\varphi_2\sqrt{\theta_2}\right)$. Previous engine investigations (such as refs. 13 to 18) have noted the failure of performance variables to generalize for all altitudes and flight Mach numbers over the range of engine speeds where sonic flow exists in the exhaust nozzle, and the studies have attributed the cause of this phenomena to low inlet Reynolds number indexes. In the larger engines, for which considerable data are available, the evaluation data seem to generalize for inlet Reynolds number indexes of about 0.5 and higher, but for indexes less than 0.5 the data do not generalize. References 13 to 18 are good examples of engine evaluations which illustrate this phenomena. In the investigation presented herein, no concerted effort was made to operate the engine at test conditions outside the operational envelope, and most of the data obtained were for the engine operating with the exhaust nozzle in the unchoked condition. Generally speaking, since the engine would have had to be operated at somewhat higher altitudes to obtain data for the lower Reynolds number indexes of interest, a broad range of inlet Reynolds number indexes was not covered. Despite this, and because there are little or no such data available for turbojet engines in this size category, those data considered applicable regarding the effects of inlet Reynolds number are presented.

A comparison of data has been made for engine operation at a nominal flight Mach number of 0.38 and for inlet Reynolds number indexes varying from about 0.35 to 1.0. Figures 13(a) to (c) illustrate the effects of varying Reynolds number indexes on the compressor characteristics, airflow, pressure ratio, and efficiency, respectively, for the

at the higher engine speeds for all Mach number conditions. For a condition of increased Mach number the engine tends to operate at lower jet exhaust (and therefore lower turbine inlet and outlet) gas temperatures (see fig. 12(a)), which results in contributing to the lower net thrust values (see fig. 12(d)). At the design cruise condition (M_0 = 0.8, 6096 m (20 000 ft)) experimental data indicated that the engine was operating at a corrected jet exhaust temperature of 808 K (1455° R) with a corrected net thrust of 1382 newtons (310 lbf) compared to 1007 K (1812° R) and 1640 newtons (368 lbf) for the corrected design values of table I. At the maximum mechanical speed of 37 000 rpm (corrected rated engine speed of 107 percent), however, the engine operated with a corrected jet exhaust temperature of 1036 K (1865° R) resulting in a corrected net thrust of 2318 newtons (520 lbf). For these maximum test conditions the thrust value was in excess of the Naval Weapons Center's cruise condition requirement by more than 669 newtons (150 lbf).

Reynolds number index correlation. - The basic objective of this investigation, with regard to engine operation, was to obtain data for sea level static conditions and for a range of simulated flight conditions within the operational envelope of figure 9 in order to allow the Naval Weapons Center to integrate this information into their demonstration test plans. The performance characteristics of this engine have been presented thus far without regard for effects on performance due to variation inlet Reynolds number index $\left(\delta_2/\varphi_2\sqrt{\theta_2}\right)$. Previous engine investigations (such as refs. 13 to 18) have noted the failure of performance variables to generalize for all altitudes and flight Mach numbers over the range of engine speeds where sonic flow exists in the exhaust nozzle, and the studies have attributed the cause of this phenomena to low inlet Reynolds number indexes. In the larger engines, for which considerable data are available, the evaluation data seem to generalize for inlet Reynolds number indexes of about 0.5 and higher, but for indexes less than 0.5 the data do not generalize. References 13 to 18 are good examples of engine evaluations which illustrate this phenomena. In the investigation presented herein, no concerted effort was made to operate the engine at test conditions outside the operational envelope, and most of the data obtained were for the engine operating with the exhaust nozzle in the unchoked condition. Generally speaking, since the engine would have had to be operated at somewhat higher altitudes to obtain data for the lower Reynolds number indexes of interest, a broad range of inlet Reynolds number indexes was not covered. Despite this, and because there are little or no such data available for turbojet engines in this size category, those data considered applicable regarding the effects of inlet Reynolds number are presented.

A comparison of data has been made for engine operation at a nominal flight Mach number of 0.38 and for inlet Reynolds number indexes varying from about 0.35 to 1.0. Figures 13(a) to (c) illustrate the effects of varying Reynolds number indexes on the compressor characteristics, airflow, pressure ratio, and efficiency, respectively, for the

engine speeds investigated. Despite a paucity of data, the figures do reflect certain definite trends. In figure 13(a) the data of corrected compressor airflow for inlet Reynolds number indexes of 0.8, 0.9, and 1.0 do generalize, while the data for the lower indexes of 0.50, 0.45, and 0.35 do not generalize as evidenced by the separate curves for each of these values. For a given engine speed, the indicated trend is that a lower value of airflow results for an inlet Reynolds number index of at least 0.5 and below. The plot of compressor pressure ratio against speed (fig. 13(b)) shows very good generalization of data over the entire range of engine speeds for all inlet Reynolds number indexes from 0.35 to 1.0. The data for compressor efficiency (fig. 13(c)) show a trend similar to that for compressor airflow in figure 13(a). In general, the trends shown in these curves are very similar to those experienced in the larger engines such as reported on in references 13 to 18. Figures 14(a) and (b) are crossplots of data presented in figures 13(a) and (c), respectively, for an engine speed of 100 percent of rated; they directly illustrate the effects of inlet Reynolds number index on both compressor airflow and compressor efficiency.

SUMMARY OF RESULTS

A small, experimental turbojet engine was fabricated according to a design which incorporated several low cost concepts and which was intended for an expendable application. The engine was subsequently subjected to a series of tests at both sea level static and simulated flight conditions. The following summarizes the results of this investigation:

1. The engine was successfully operated at both sea level static and simulated flight conditions within the intended operational envelope. Testing conditions included representative altitudes as high as 9144 meters (30 000 ft) and flight Mach numbers as high as 1.24.

2. At its design speed the engine was unable to produce the required thrust values of 2669 newtons (600 lbf) at sea level static operation and 1557 newtons (350 lbf) at its design cruise condition of $M_0 = 0.8$ and 6096 meters (20 000 ft). Unexpectedly low compressor efficiencies (0.69 to 0.74) were undoubtedly a major contributing factor for the low thrust outputs. In addition, the poor compressor performance resulted in a relatively small stall margin for operation at sea level static conditions. Operation at a condition of 107 percent of the rated corrected engine speed, however, did produce thrusts well in excess of the required values. For this overspeed condition, the engine produced a net thrust of 3118 newtons (701 lbf) at sea level static and 2318 newtons (520 lbf) at its simulated cruise condition.

engine speeds investigated. Despite a paucity of data, the figures do reflect certain definite trends. In figure 13(a) the data of corrected compressor airflow for inlet Reynolds number indexes of 0.8, 0.9, and 1.0 do generalize, while the data for the lower indexes of 0.50, 0.45, and 0.35 do not generalize as evidenced by the separate curves for each of these values. For a given engine speed, the indicated trend is that a lower value of airflow results for an inlet Reynolds number index of at least 0.5 and below. The plot of compressor pressure ratio against speed (fig. 13(b)) shows very good generalization of data over the entire range of engine speeds for all inlet Reynolds number indexes from 0.35 to 1.0. The data for compressor efficiency (fig. 13(c)) show a trend similar to that for compressor airflow in figure 13(a). In general, the trends shown in these curves are very similar to those experienced in the larger engines such as reported on in references 13 to 18. Figures 14(a) and (b) are crossplots of data presented in figures 13(a) and (c), respectively, for an engine speed of 100 percent of rated; they directly illustrate the effects of inlet Reynolds number index on both compressor airflow and compressor efficiency.

SUMMARY OF RESULTS

A small, experimental turbojet engine was fabricated according to a design which incorporated several low cost concepts and which was intended for an expendable application. The engine was subsequently subjected to a series of tests at both sea level static and simulated flight conditions. The following summarizes the results of this investigation:

1. The engine was successfully operated at both sea level static and simulated flight conditions within the intended operational envelope. Testing conditions included representative altitudes as high as 9144 meters (30 000 ft) and flight Mach numbers as high as 1.24.

2. At its design speed the engine was unable to produce the required thrust values of 2669 newtons (600 lbf) at sea level static operation and 1557 newtons (350 lbf) at its design cruise condition of $M_0 = 0.8$ and 6096 meters (20 000 ft). Unexpectedly low compressor efficiencies (0.69 to 0.74) were undoubtedly a major contributing factor for the low thrust outputs. In addition, the poor compressor performance resulted in a relatively small stall margin for operation at sea level static conditions. Operation at a condition of 107 percent of the rated corrected engine speed, however, did produce thrusts well in excess of the required values. For this overspeed condition, the engine produced a net thrust of 3118 newtons (701 lbf) at sea level static and 2318 newtons (520 lbf) at its simulated cruise condition.

3. The engine demonstrated its capability of transient operation by successfully completing a series of acceleration-deceleration tests at sea level static conditions without encountering a surge or flameout condition. These tests included a snap acceleration (throttle advance in less than 1/2 sec) from about 26 000 to 37 000 rpm (approximately 75 to 105 percent of its rated engine speed).

4. The engine successfully completed a 1-hour continuous steady-state test at sea level static for the maximum speed condition of 37 000 rpm; it thereby proved its capability for a proposed mission having a duration of 20 minutes.

5. The engine successfully completed several starts from a windmilling operation at various simulated flight conditions within its proposed operational envelope to demonstrate its capability for an intended air launch.

6. Data obtained from this investigation indicate that the effect on the engine's compressor characteristics resulting from varying the inlet Reynolds number index produced trends similar to those previously established for much larger engines. For a nominal Mach number of 0.38, the data generalize for inlet Reynolds number indexes of 0.5 or greater, while at lower indexes the data do not generalize.

Lewis Research Center,
National Aeronautics and Space Administration,
Cleveland, Ohio, July 22, 1976,
505-05.

REFERENCES

1. Cummings, Robert L.; and Gold, Harold: Concepts for Cost Reduction in Turbine Engines for General Aviation. NASA TM X-52951, 1971.
2. Cummings, Robert L.: Experience with Low Cost Engines. NASA TM X-68085, 1972.
3. Gold, Harold: A Simplified Fuel Control Approach for Low Cost Aircraft Gas Turbines. NASA TM X-68229, 1973.
4. Fear, James S.: Performance of an Annular Combustor Designed for a Low Cost Turbojet Engine. NASA TM X-2857, 1973.
5. Kofskey, Milton G.; Roelke, Richard J.; and Haas, Jeffrey E.: Turbine for a Low Cost Turbojet Engine. I - Design and Cold Air Performance. NASA TN D-7625, 1974.

3. The engine demonstrated its capability of transient operation by successfully completing a series of acceleration-deceleration tests at sea level static conditions without encountering a surge or flameout condition. These tests included a snap acceleration (throttle advance in less than 1/2 sec) from about 26 000 to 37 000 rpm (approximately 75 to 105 percent of its rated engine speed).

4. The engine successfully completed a 1-hour continuous steady-state test at sea level static for the maximum speed condition of 37 000 rpm; it thereby proved its capability for a proposed mission having a duration of 20 minutes.

5. The engine successfully completed several starts from a windmilling operation at various simulated flight conditions within its proposed operational envelope to demonstrate its capability for an intended air launch.

6. Data obtained from this investigation indicate that the effect on the engine's compressor characteristics resulting from varying the inlet Reynolds number index produced trends similar to those previously established for much larger engines. For a nominal Mach number of 0.38, the data generalize for inlet Reynolds number indexes of 0.5 or greater, while at lower indexes the data do not generalize.

Lewis Research Center,
National Aeronautics and Space Administration,
Cleveland, Ohio, July 22, 1976,
505-05.

REFERENCES

1. Cummings, Robert L.; and Gold, Harold: Concepts for Cost Reduction in Turbine Engines for General Aviation. NASA TM X-52951, 1971.
2. Cummings, Robert L.: Experience with Low Cost Engines. NASA TM X-68085, 1972.
3. Gold, Harold: A Simplified Fuel Control Approach for Low Cost Aircraft Gas Turbines. NASA TM X-68229, 1973.
4. Fear, James S.: Performance of an Annular Combustor Designed for a Low Cost Turbojet Engine. NASA TM X-2857, 1973.
5. Kofskey, Milton G.; Roelke, Richard J.; and Haas, Jeffrey E.: Turbine for a Low Cost Turbojet Engine. I - Design and Cold Air Performance. NASA TN D-7625, 1974.

6. Roelke, Richard J.; and Stewart, Warner L.: Turbojet and Turbofan Cycle Considerations and Engine Configuration for Application in Lightweight Aircraft. NASA TM X-1624, 1968.

7. Kraft, Gerald A.; and Miller, Brent A.: Off-Design Theoretical Performance of Three Turbofan Engines for Light Subsonic Aircraft. NASA TM X-52469, 1968.

8. Dugan, James F., Jr : Theoretical Performance of Turbojet Engine for Light Subsonic Aircraft. NASA TM X-52538, 1969.

9. Dengler, Robert P.; and Macioce, Lawrence E.: Small, Low-Cost, Expendable Turbojet Engine. Part I - Design, Fabrication, and Preliminary Testing. NASA TM X-3392, 1976.

10. Dengler, R. P.: Experience with Integrally Cast Compressor and Turbine Components for a Small, Low-Cost, Expendable-Type Turbojet Engine. SAE Paper 751048, Nov. 1975.

11. Central Automatic Data Processing System. NACA TN 4212, 1958.

12. Seldner, Kurt, et al.: Performance and Control Study of a Low Pressure-Ratio Turbojet Engine for a Drone Aircraft. NASA TM X-2537, 1972.

13. Vincent, K. R.; and Gale, B. M.: Altitude Performance of J35-A-17 Turbojet Engine in an Altitude Chamber. NACA RM E50I15, 1951.

14. Fleming, William A.: Effects of Altitude on Turbojet Engine Performance. NACA RM E51J15, 1951.

15. Walker, Curtis L.; Huntley, Sidney C.; and Braithwaite, Willis M.: Component and Overall Performance Evaluation of an Axial-Flow Turbojet Engine over a Range of Engine-Inlet Reynolds Numbers. NACA RM E52B08, 1952.

16. Walker, Curtis L.; Braithwaite, Willis M.; and Fenn, David B.: Component and Overall Performance Evaluation of a J47-GE-25 Turbojet Engine over a Range of Engine-Inlet Reynolds Number Indices. NACA RM E52L16, 1953.

17. Antl, Robert J.; and Burley, Richard R.: Steady-State Airflow and Afterburning Performance Characteristics of Four J-85-GE-13 Turbojet Engines. NASA TM X-1742, 1970.

18. Antl, Robert J.; Smith, John M.; and Riddlebaugh, Stephen M.: Effect of Screen-Induced Inlet-Flow Distortions on Performance and Stall Characteristics of an Afterburner Equipped Turbofan Engine. NASA TM X-2242, 1971.

6. Roelke, Richard J.; and Stewart, Warner L.: Turbojet and Turbofan Cycle Considerations and Engine Configuration for Application in Lightweight Aircraft. NASA TM X-1624, 1968.

7. Kraft, Gerald A.; and Miller, Brent A.: Off-Design Theoretical Performance of Three Turbofan Engines for Light Subsonic Aircraft. NASA TM X-52469, 1968.

8. Dugan, James F., Jr : Theoretical Performance of Turbojet Engine for Light Subsonic Aircraft. NASA TM X-52538, 1969.

9. Dengler, Robert P.; and Macioce, Lawrence E.: Small, Low-Cost, Expendable Turbojet Engine. Part I - Design, Fabrication, and Preliminary Testing. NASA TM X-3392, 1976.

10. Dengler, R. P.: Experience with Integrally Cast Compressor and Turbine Components for a Small, Low-Cost, Expendable-Type Turbojet Engine. SAE Paper 751048, Nov. 1975.

11. Central Automatic Data Processing System. NACA TN 4212, 1958.

12. Seldner, Kurt, et al.: Performance and Control Study of a Low Pressure-Ratio Turbojet Engine for a Drone Aircraft. NASA TM X-2537, 1972.

13. Vincent, K. R.; and Gale, B. M.: Altitude Performance of J35-A-17 Turbojet Engine in an Altitude Chamber. NACA RM E50I15, 1951.

14. Fleming, William A.: Effects of Altitude on Turbojet Engine Performance. NACA RM E51J15, 1951.

15. Walker, Curtis L.; Huntley, Sidney C.; and Braithwaite, Willis M.: Component and Overall Performance Evaluation of an Axial-Flow Turbojet Engine over a Range of Engine-Inlet Reynolds Numbers. NACA RM E52B08, 1952.

16. Walker, Curtis L.; Braithwaite, Willis M.; and Fenn, David B.: Component and Overall Performance Evaluation of a J47-GE-25 Turbojet Engine over a Range of Engine-Inlet Reynolds Number Indices. NACA RM E52L16, 1953.

17. Antl, Robert J.; and Burley, Richard R.: Steady-State Airflow and Afterburning Performance Characteristics of Four J-85-GE-13 Turbojet Engines. NASA TM X-1742, 1970.

18. Antl, Robert J.; Smith, John M.; and Riddlebaugh, Stephen M.: Effect of Screen-Induced Inlet-Flow Distortions on Performance and Stall Characteristics of an Afterburner Equipped Turbofan Engine. NASA TM X-2242, 1971.

14

TABLE I. - ENGINE DESIGN VALUES FOR OPERATING CHARACTERISTICS

AND INTERNAL GAS CONDITIONS

[Values in uncorrected form; i.e., not generalized to sea level conditions.]

Condition	Sea level [illegible]ic	Cruise
Altitude, m (ft)	'0)	6096 (20 000)
Mach number	(0)	0.8
Ambient temperature, K (^{o}R)	288 \ 9)	249 (448)
Power setting	Max.	Cruise
Speed, rpm	35 170	34 700
Inlet pressure ratio	0.95	0.99
Compressor:		
Airflow, kg/sec (lbm/sec)	4.387 (9.672)	3.24 (7.14)
Inlet temperature, K (^{o}R)	288 (519)	281 (505)
Outlet temperature, K (^{o}R)	455 (819)	439 (791)
Inlet pressure, N/m^2 (psia)	96 530 (14.0)	70 330 (10.2)
Pressure ratio	4.0	4.0
Adiabatic efficiency	0.83	0.85
Outlet pressure, N/m^2 (psia)	384 740 (55.8)	281 320 (40.8)
Combustor:		
Adiabatic efficiency	0.96	0.96
Outlet temperature, K (^{o}R)	1119 (2015)	1089 (1960)
Outlet pressure, N/m^2 (psia)	360 610 (52.3)	263 390 (38.2)
Heating value, J/kg (Btu/lbm)	4.33×10^7 (18 640)	4.33×10^7 (18 640)
Burner pressure ratio	0.937	0.937
Fuel-air ratio	0.0183	0.0172
Turbine:		
Adiabatic efficiency	0.88	0.88
Pressure ratio	1.881	1.854
Mass flow, kg/sec (lbm/sec)	4.468 (9.849)	3.296 (7.267)
Outlet temperature, K (^{o}R)	979 (1762)	954 (1718)
Outlet pressure, N/m^2 (psia)	191 680 (27.8)	142 040 (20.6)
Nozzle:		
Nozzle pressure ratio	1.891	3.048
Nozzle area, m^2 (ft^2)	0.0179 (0.193)	0.0179 (0.193)
Thrust coefficient	0.99	0.99
Performance:		
Net thrust, N (lbf)	2543 (571.8)	1562 (351.2)
Specific fuel consumption, (kg/lb)/N((lb/hr)/lb)	1.114	1.300

TABLE I. - ENGINE DESIGN VALUES FOR OPERATING CHARACTERISTICS

AND INTERNAL GAS CONDITIONS

[Values in uncorrected form; i.e., not generalized to sea level conditions.]

Condition	Sea level [illegible]ic	Cruise
Altitude, m (ft)	'0)	6096 (20 000)
Mach number	(0)	0.8
Ambient temperature, K (^{o}R)	288 \ 9)	249 (448)
Power setting	Max.	Cruise
Speed, rpm	35 170	34 700
Inlet pressure ratio	0.95	0.99
Compressor:		
Airflow, kg/sec (lbm/sec)	4.387 (9.672)	3.24 (7.14)
Inlet temperature, K (^{o}R)	288 (519)	281 (505)
Outlet temperature, K (^{o}R)	455 (819)	439 (791)
Inlet pressure, N/m^2 (psia)	96 530 (14.0)	70 330 (10.2)
Pressure ratio	4.0	4.0
Adiabatic efficiency	0.83	0.85
Outlet pressure, N/m^2 (psia)	384 740 (55.8)	281 320 (40.8)
Combustor:		
Adiabatic efficiency	0.96	0.96
Outlet temperature, K (^{o}R)	1119 (2015)	1089 (1960)
Outlet pressure, N/m^2 (psia)	360 610 (52.3)	263 390 (38.2)
Heating value, J/kg (Btu/lbm)	4.33×10^7 (18 640)	4.33×10^7 (18 640)
Burner pressure ratio	0.937	0.937
Fuel-air ratio	0.0183	0.0172
Turbine:		
Adiabatic efficiency	0.88	0.88
Pressure ratio	1.881	1.854
Mass flow, kg/sec (lbm/sec)	4.468 (9.849)	3.296 (7.267)
Outlet temperature, K (^{o}R)	979 (1762)	954 (1718)
Outlet pressure, N/m^2 (psia)	191 680 (27.8)	142 040 (20.6)
Nozzle:		
Nozzle pressure ratio	1.891	3.048
Nozzle area, m^2 (ft^2)	0.0179 (0.193)	0.0179 (0.193)
Thrust coefficient	0.99	0.99
Performance:		
Net thrust, N (lbf)	2543 (571.8)	1562 (351.2)
Specific fuel consumption, (kg/lb)/N((lb/hr)/lb)	1.114	1.300

15

TABLE II. - COMPARISON OF SELECTED ENGINE PERFORMANCE CHARACTERISTICS AT SEA LEVEL STATIC CONDITIONS

	Corrected engine speed, $\%N_R/\sqrt{\theta_2}$, percent of rated	Compressor pressure ratio, $P_{t,3}/P_{t,2}$	Compressor temperature ratio, $T_{t,3}/T_{t,2}$	Corrected compressor airflow, $\frac{W_2\sqrt{\theta_2}}{\delta_2}$, kg/sec (lbm/sec)	Compressor efficiency, η_c	Corrected jet exhaust temperature, $T_{t,6}/\theta_2$, K ($^\circ$R)	Engine pressure ratio, $P_{t,6}/P_{t,2}$	Engine temperature ratio, $T_{t,6}/T_{t,2}$	Corrected net thrust, F/δ_2, N (lbf)	Corrected fuel flow, $\frac{W_f}{\delta_2\sqrt{\theta_2}}$, kg/hr (lbm/hr)
Design	100 (35 170 rpm)	4.0	1.58	4.60 (10.15)	0.83	979 (1762)	1.99	3.39	2669 (600)	303 (669)
Engine data	100	3.68	1.61	4.45 (9.81)	.738	961 (1730)	1.60	3.33	2230 (501)	293 (645)
Engine data	107	4.32	1.74	4.89 (10.79)	.702	1123 (2021)	1.86	4.07	3120 (701)	435 (958)

TABLE III. - SUMMARY OF STEADY-STATE OPERATING CONDITIONS

FOR SIMULATED FLIGHT DATA

Altitude		Flight Mach number, M_0	Inlet Reynolds number index, $\delta_2/\varphi_2\sqrt{\theta_2}$
m	ft		
610	2 000	0.38, 0.68	0.99, 1.15
1524	5 000	0.24, 0.38, 0.61, 0.68	0.88, 0.91, 1.04, 1.17
3048	10 000	0.24, 0.38, 0.50	0.76, 0.80, 0.84
4572	15 000	0.17, 0.50, 0.68, 0.82, 1.07	0.65, 0.72, 0.79, 0.85, 1.06
6096	20 000	0.38, 0.50, 0.68, 0.82	0.51, 0.62, 0.67, 0.75
6706	22 000	0.38	0.47
7315	24 000	0.38	0.43
7620	25 000	0.68, 0.82, 1.08, 1.24	0.57, 0.62, 0.75, 0.86
7925	26 000	0.38	0.39
8534	28 000	0.38	0.36
9144	30 000	0.51, 0.82, 1.09, 1.24	0.35, 0.45, 0.61, 0.74

TABLE II. - COMPARISON OF SELECTED ENGINE PERFORMANCE CHARACTERISTICS AT SEA LEVEL STATIC CONDITIONS

	Corrected engine speed, $\%N_R/\sqrt{\theta_2}$, percent of rated	Compressor pressure ratio, $P_{t,3}/P_{t,2}$	Compressor temperature ratio, $T_{t,3}/T_{t,2}$	Corrected compressor airflow, $\frac{W_2\sqrt{\theta_2}}{\delta_2}$, kg/sec (lbm/sec)	Compressor efficiency, η_c	Corrected jet exhaust temperature, $T_{t,6}/\theta_2$, K ($^\circ$R)	Engine pressure ratio, $P_{t,6}/P_{t,2}$	Engine temperature ratio, $T_{t,6}/T_{t,2}$	Corrected net thrust, F/δ_2, N (lbf)	Corrected fuel flow, $\frac{W_f}{\delta_2\sqrt{\theta_2}}$, kg/hr (lbm/hr)
Design	100 (35 170 rpm)	4.0	1.58	4.60 (10.15)	0.83	979 (1762)	1.99	3.39	2669 (600)	303 (669)
Engine data	100	3.68	1.61	4.45 (9.81)	.738	961 (1730)	1.60	3.33	2230 (501)	293 (645)
Engine data	107	4.32	1.74	4.89 (10.79)	.702	1123 (2021)	1.86	4.07	3120 (701)	435 (958)

TABLE III. - SUMMARY OF STEADY-STATE OPERATING CONDITIONS

FOR SIMULATED FLIGHT DATA

Altitude		Flight Mach number, M_0	Inlet Reynolds number index, $\delta_2/\varphi_2\sqrt{\theta_2}$
m	ft		
610	2 000	0.38, 0.68	0.99, 1.15
1524	5 000	0.24, 0.38, 0.61, 0.68	0.88, 0.91, 1.04, 1.17
3048	10 000	0.24, 0.38, 0.50	0.76, 0.80, 0.84
4572	15 000	0.17, 0.50, 0.68, 0.82, 1.07	0.65, 0.72, 0.79, 0.85, 1.06
6096	20 000	0.38, 0.50, 0.68, 0.82	0.51, 0.62, 0.67, 0.75
6706	22 000	0.38	0.47
7315	24 000	0.38	0.43
7620	25 000	0.68, 0.82, 1.08, 1.24	0.57, 0.62, 0.75, 0.86
7925	26 000	0.38	0.39
8534	28 000	0.38	0.36
9144	30 000	0.51, 0.82, 1.09, 1.24	0.35, 0.45, 0.61, 0.74

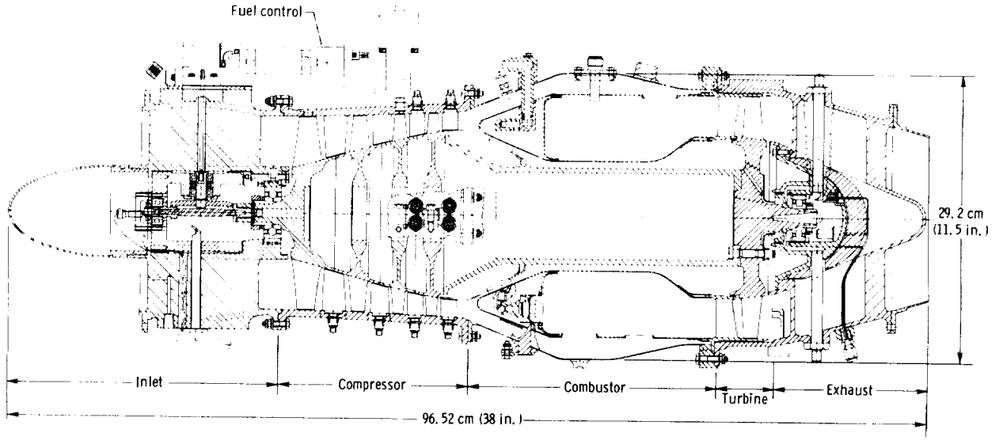

Figure 1. - Cross-sectional view of engine design.

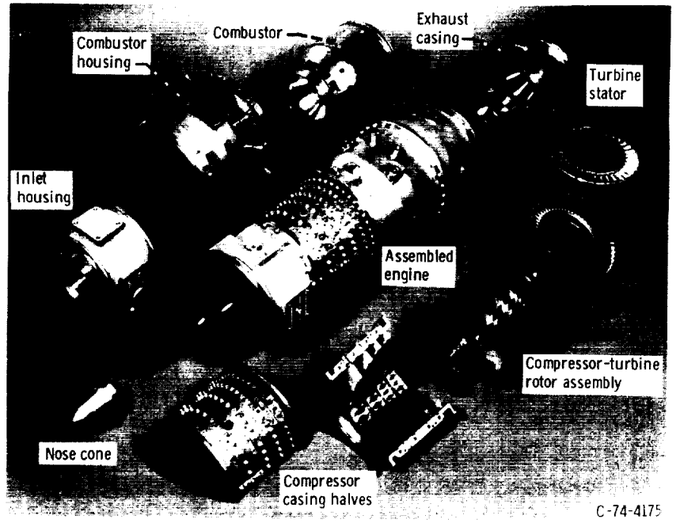

Figure 2. - Assembled engine and its major components.

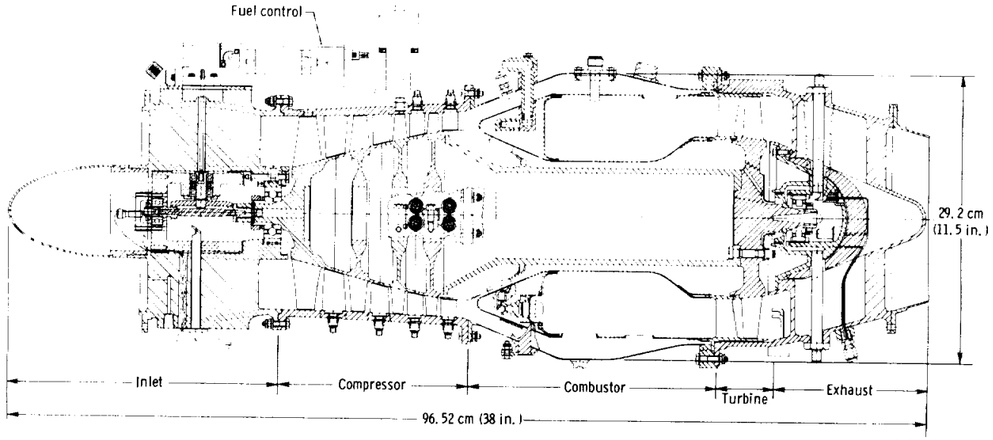

Figure 1. - Cross-sectional view of engine design.

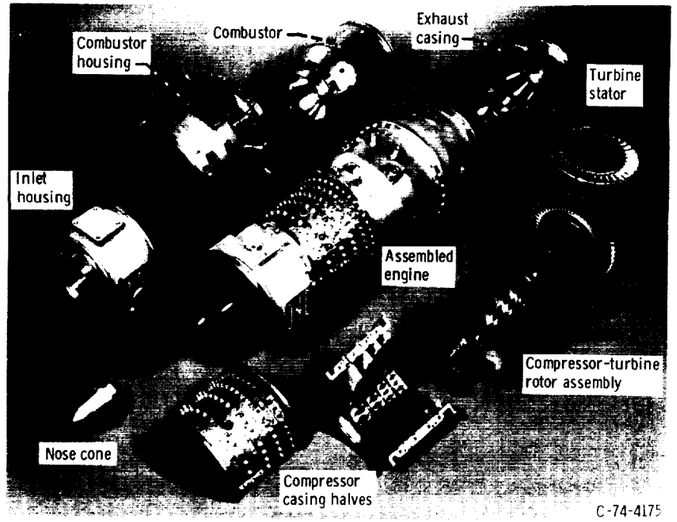

Figure 2. - Assembled engine and its major components.

17

(a) SPL facility (sea level static testing).

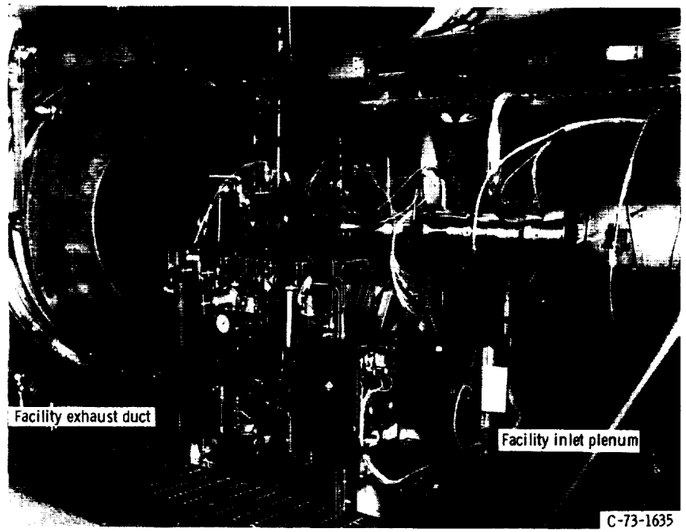

(b) PSL facility (altitude test chamber).

Figure 3. - Engine installations.

(a) SPL facility (sea level static testing).

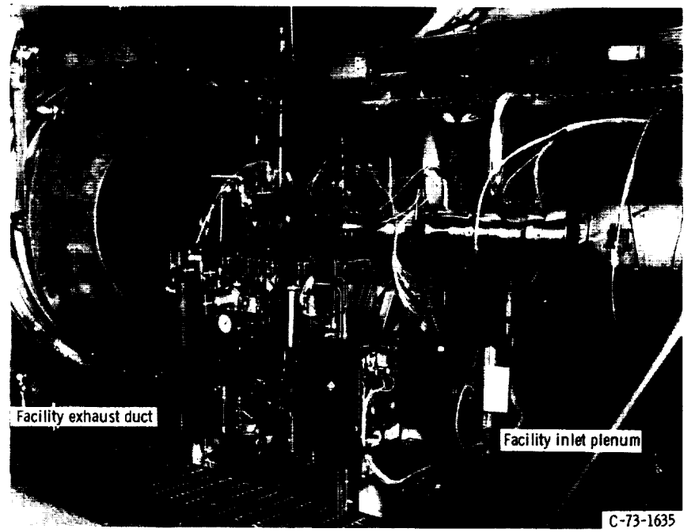

(b) PSL facility (altitude test chamber).

Figure 3. - Engine installations.

18

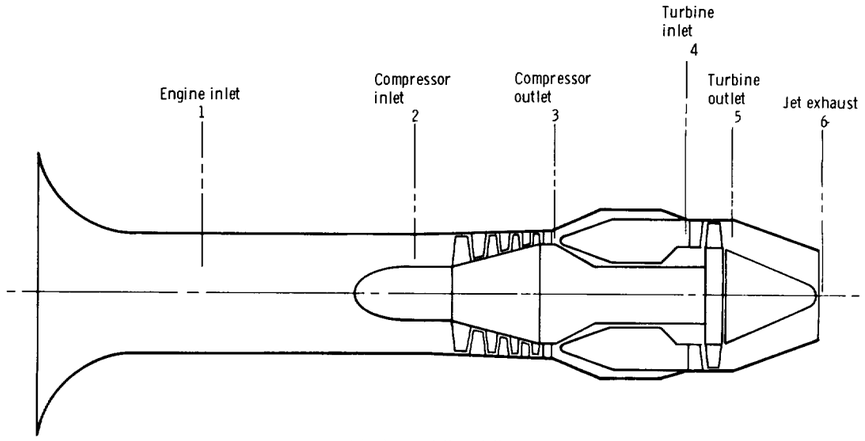

(a) Instrumentation stations.

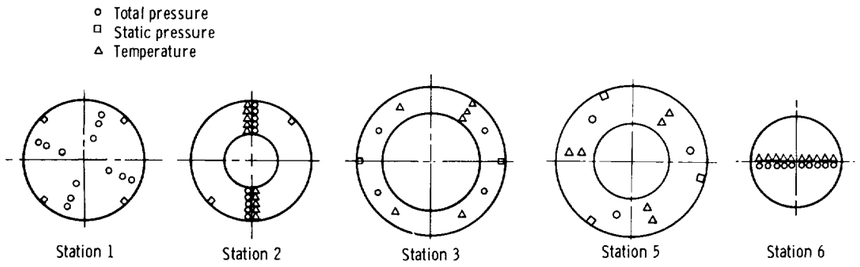

(b) Individual station layout (viewed looking upstream).

Figure 4. - Engine instrumentation layout.

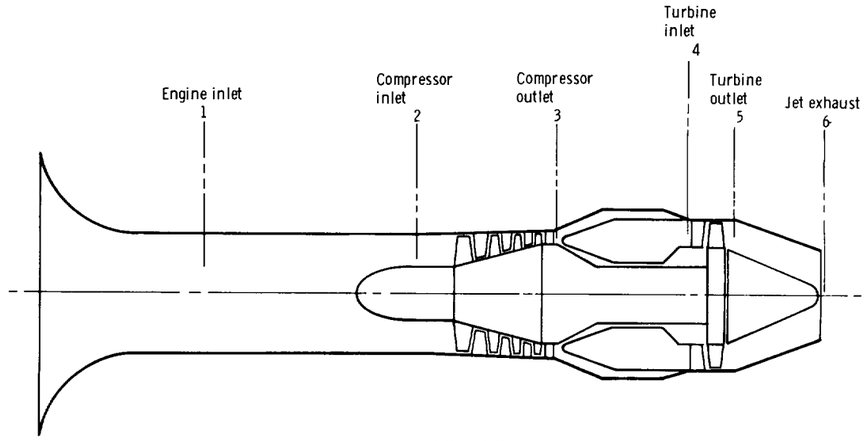

(a) Instrumentation stations.

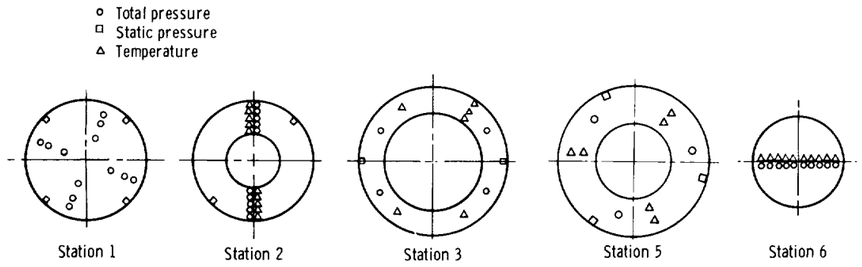

(b) Individual station layout (viewed looking upstream).

Figure 4. - Engine instrumentation layout.

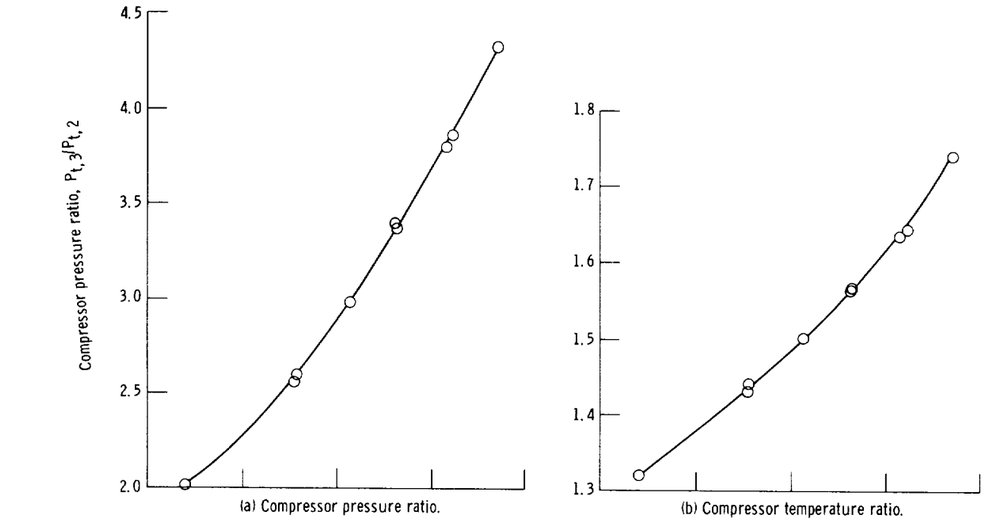

(a) Compressor pressure ratio.

(b) Compressor temperature ratio.

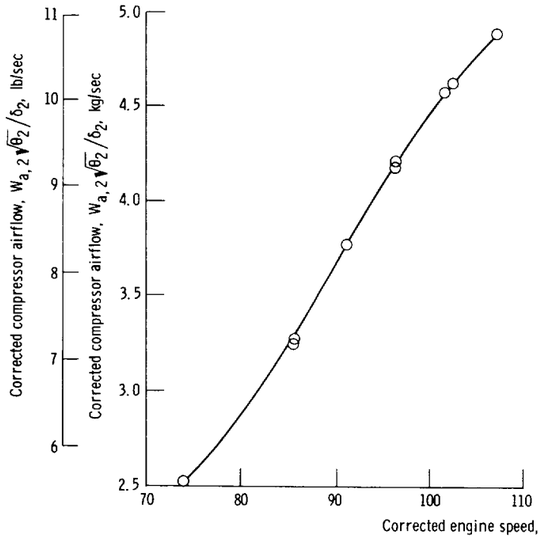

(c) Corrected compressor airflow.

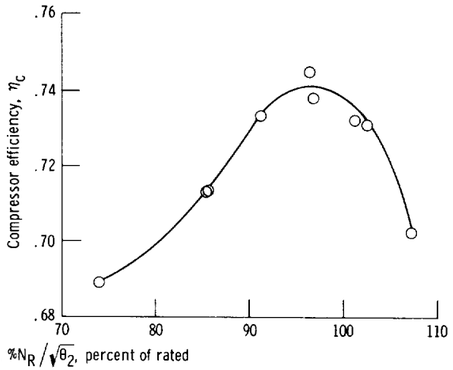

(d) Compressor efficiency.

Figure 5. - Compressor performance characteristics at sea level static conditions. Rated engine speed, 35 170 rpm.

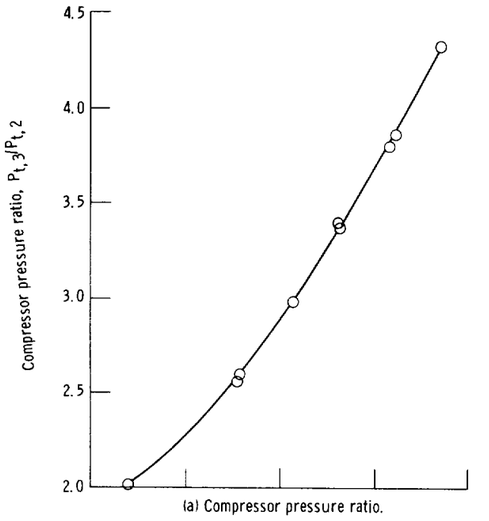

(a) Compressor pressure ratio.

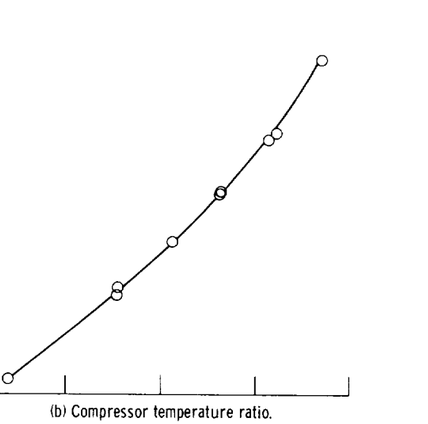

(b) Compressor temperature ratio.

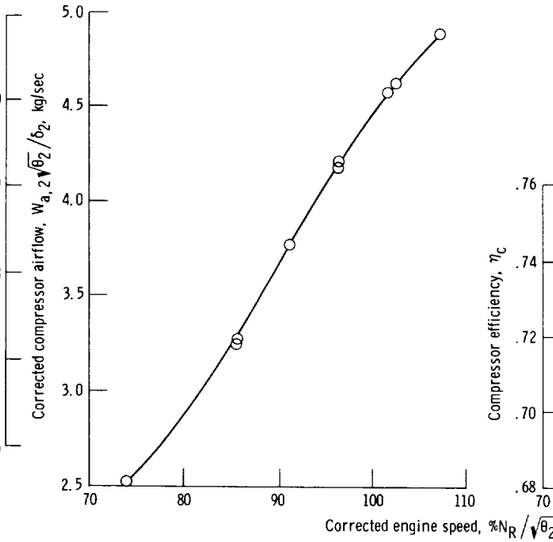

(c) Corrected compressor airflow.

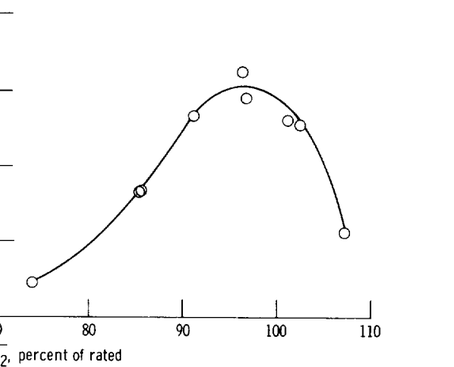

(d) Compressor efficiency.

Figure 5. - Compressor performance characteristics at sea level static conditions. Rated engine speed, 35 170 rpm.

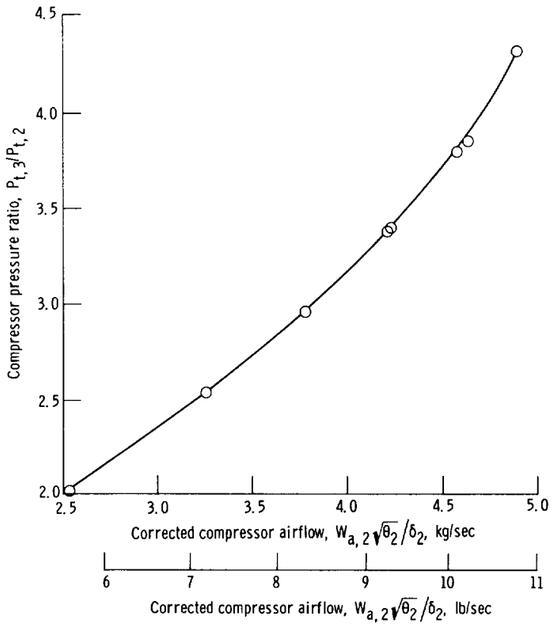

(e) Normal engine operating line for sea level static conditions.

Figure 5. - Concluded.

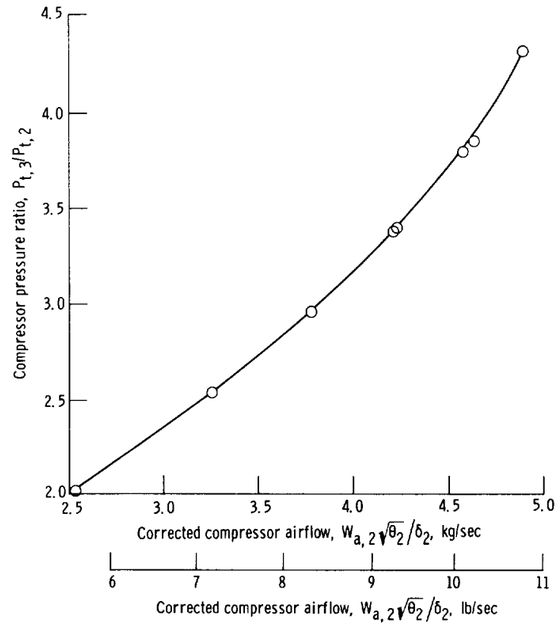

(e) Normal engine operating line for sea level static conditions.

Figure 5. - Concluded.

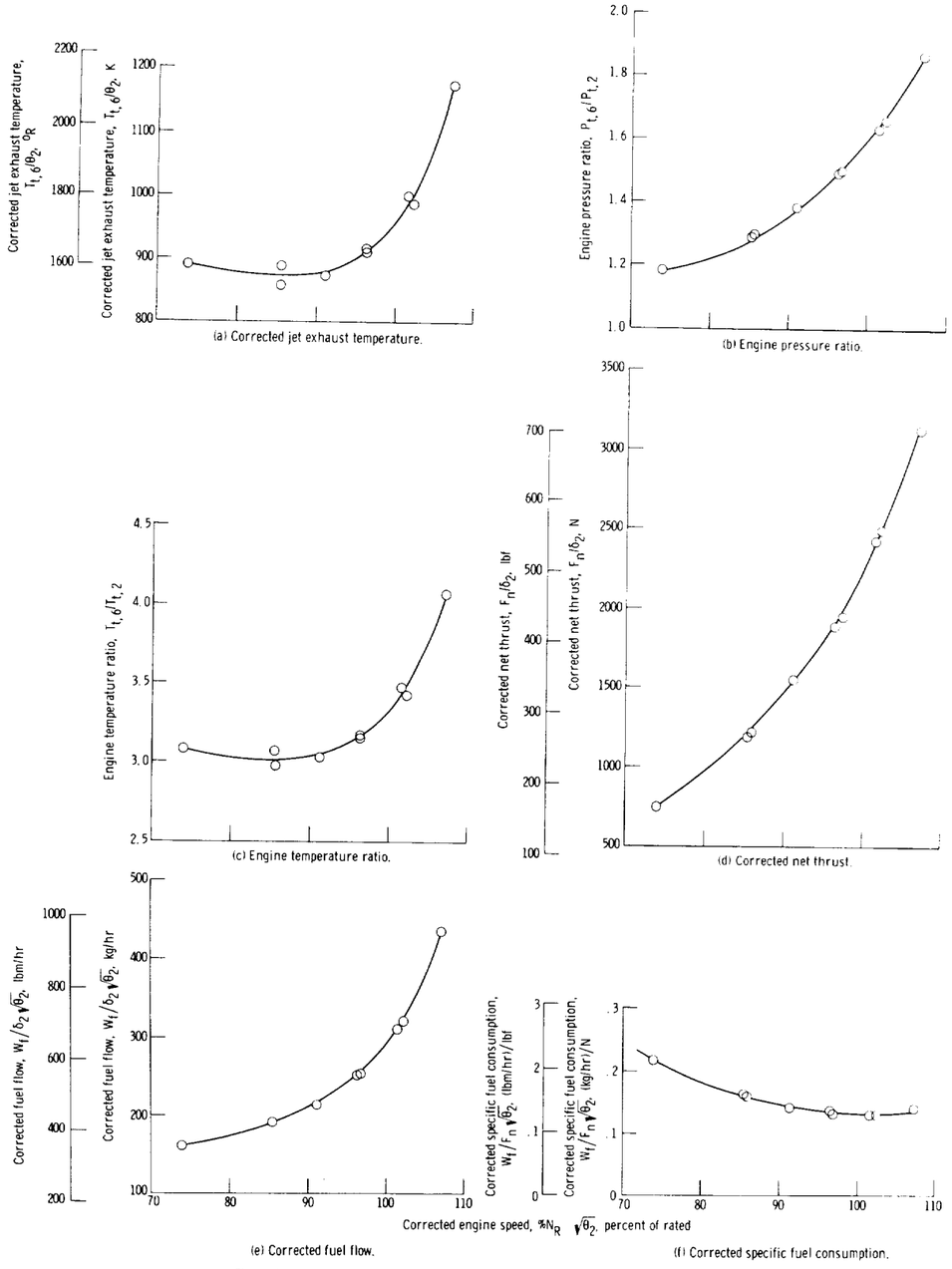

Figure 6. - Engine performance characteristics at sea level static conditions. Rated engine speed, 35 170 rpm.

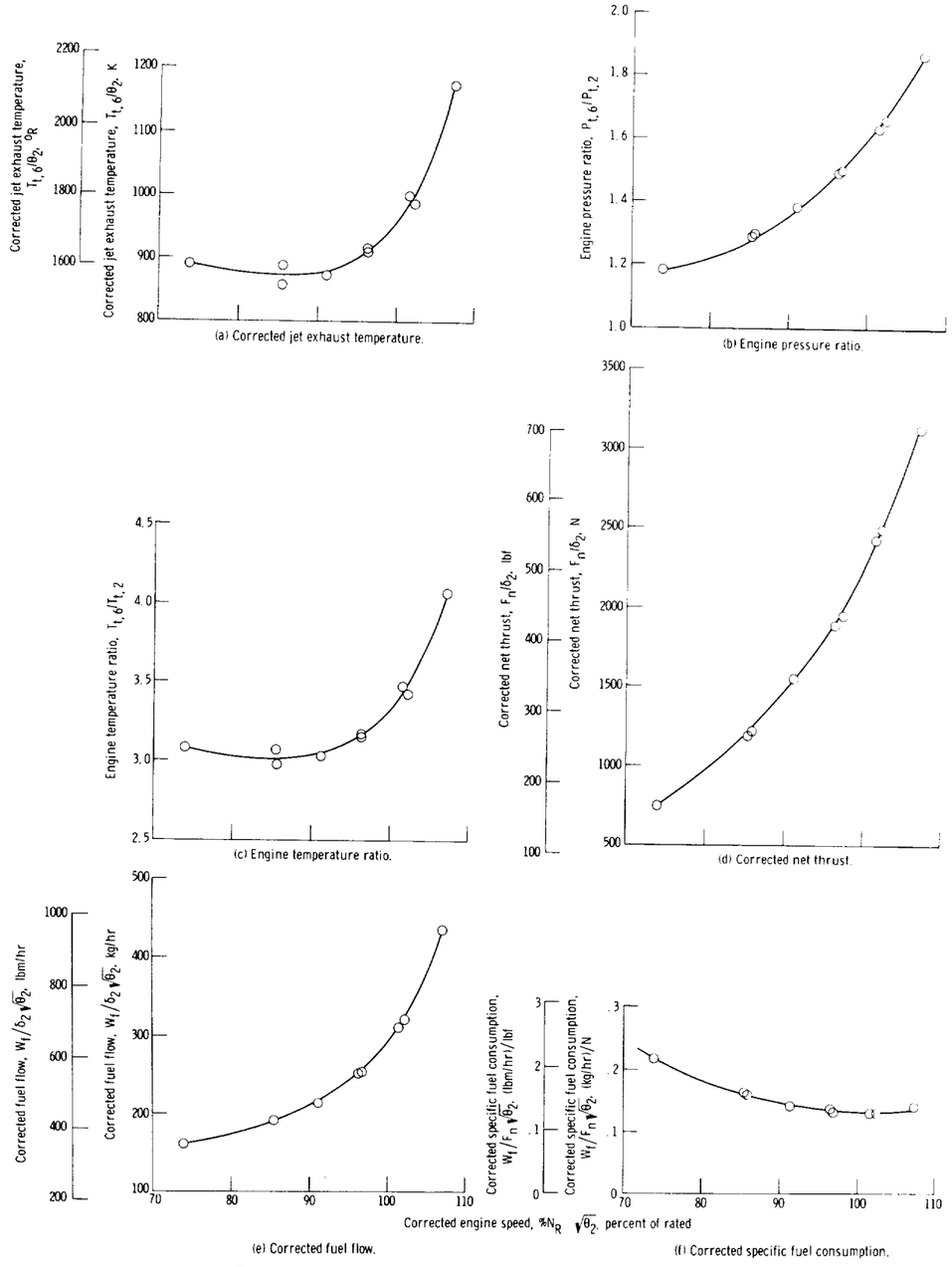
Figure 6. - Engine performance characteristics at sea level static conditions. Rated engine speed, 35 170 rpm.

22

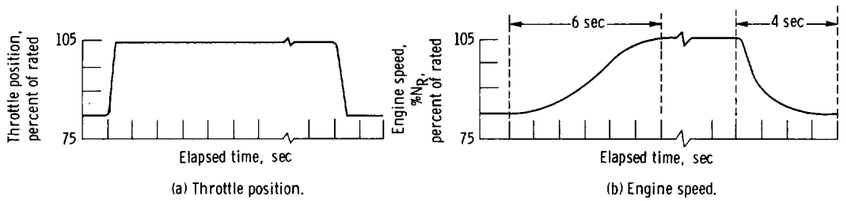

(a) Throttle position. (b) Engine speed.

Figure 7. - Fuel control response characteristics for a rapid acceleration and deceleration at sea level static conditions. Rated engine speed, 35 170 rpm.

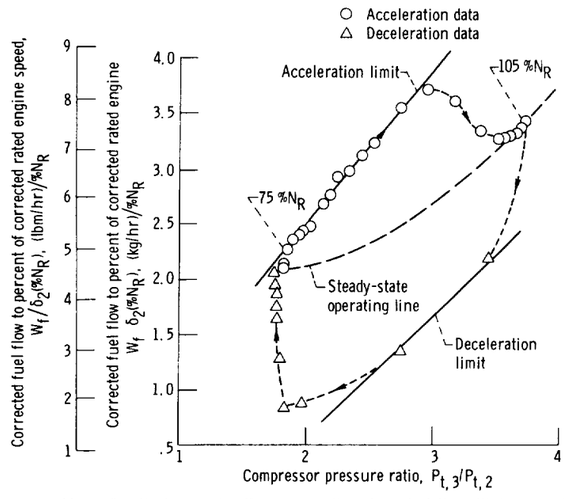

Figure 8. - Engine acceleration-deceleration characteristics with integrated fuel control. Generalized fuel speed parameter plotted as function of compressor pressure ratio. Rated engine speed, 35 170 rpm.

Throttle position, percent of rated
105
75
Elapsed time, sec
Engine speed, %N_R, percent of rated
6 sec
4 sec
105
75
Elapsed time, sec

(a) Throttle position. (b) Engine speed.

Figure 7. - Fuel control response characteristics for a rapid acceleration and deceleration at sea level static conditions. Rated engine speed, 35 170 rpm.

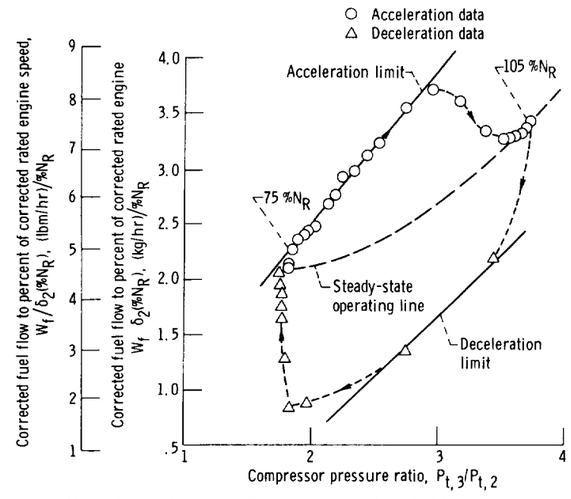

Figure 8. - Engine acceleration-deceleration characteristics with integrated fuel control. Generalized fuel speed parameter plotted as function of compressor pressure ratio. Rated engine speed, 35 170 rpm.

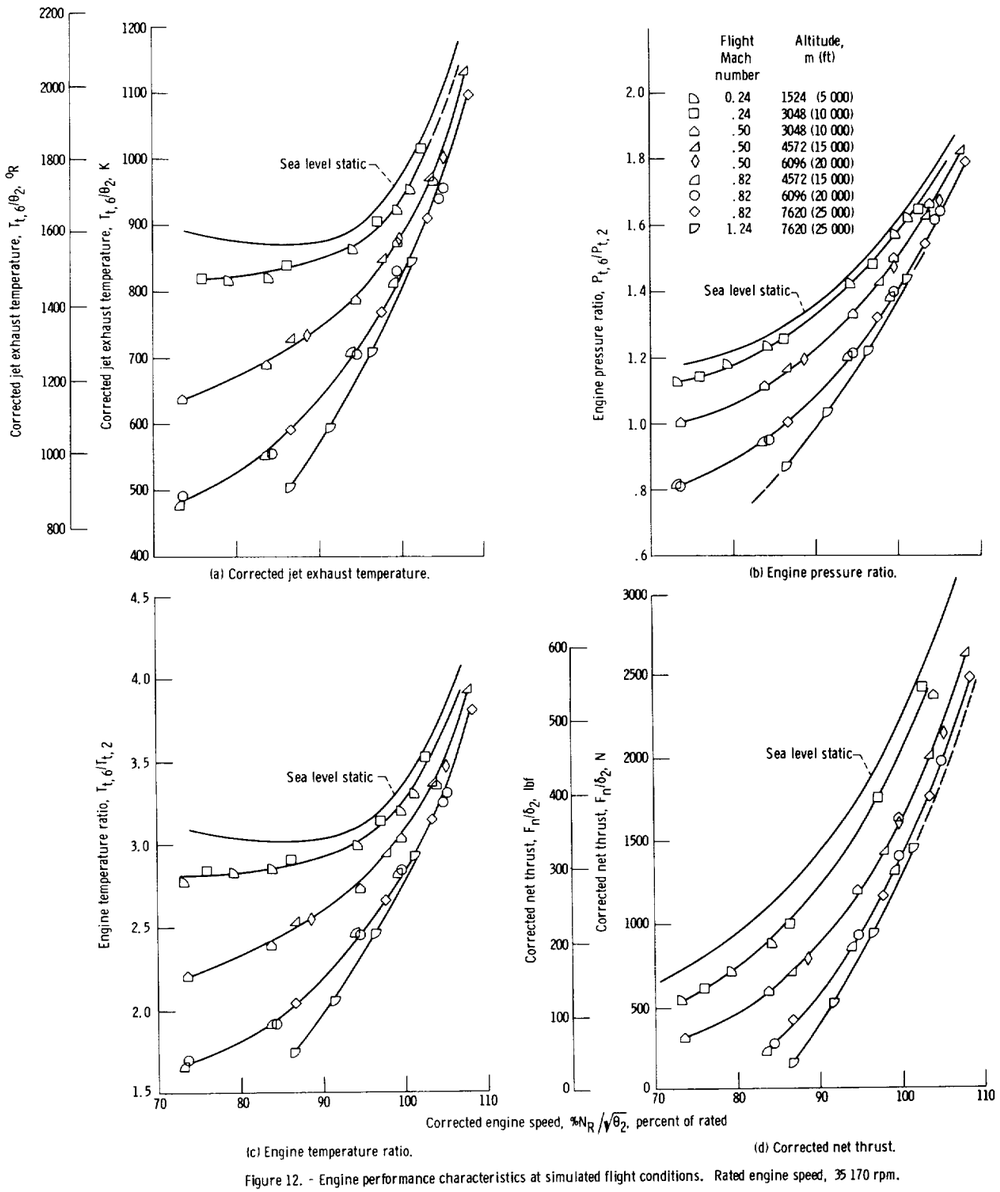

Figure 12. - Engine performance characteristics at simulated flight conditions. Rated engine speed, 35 170 rpm.

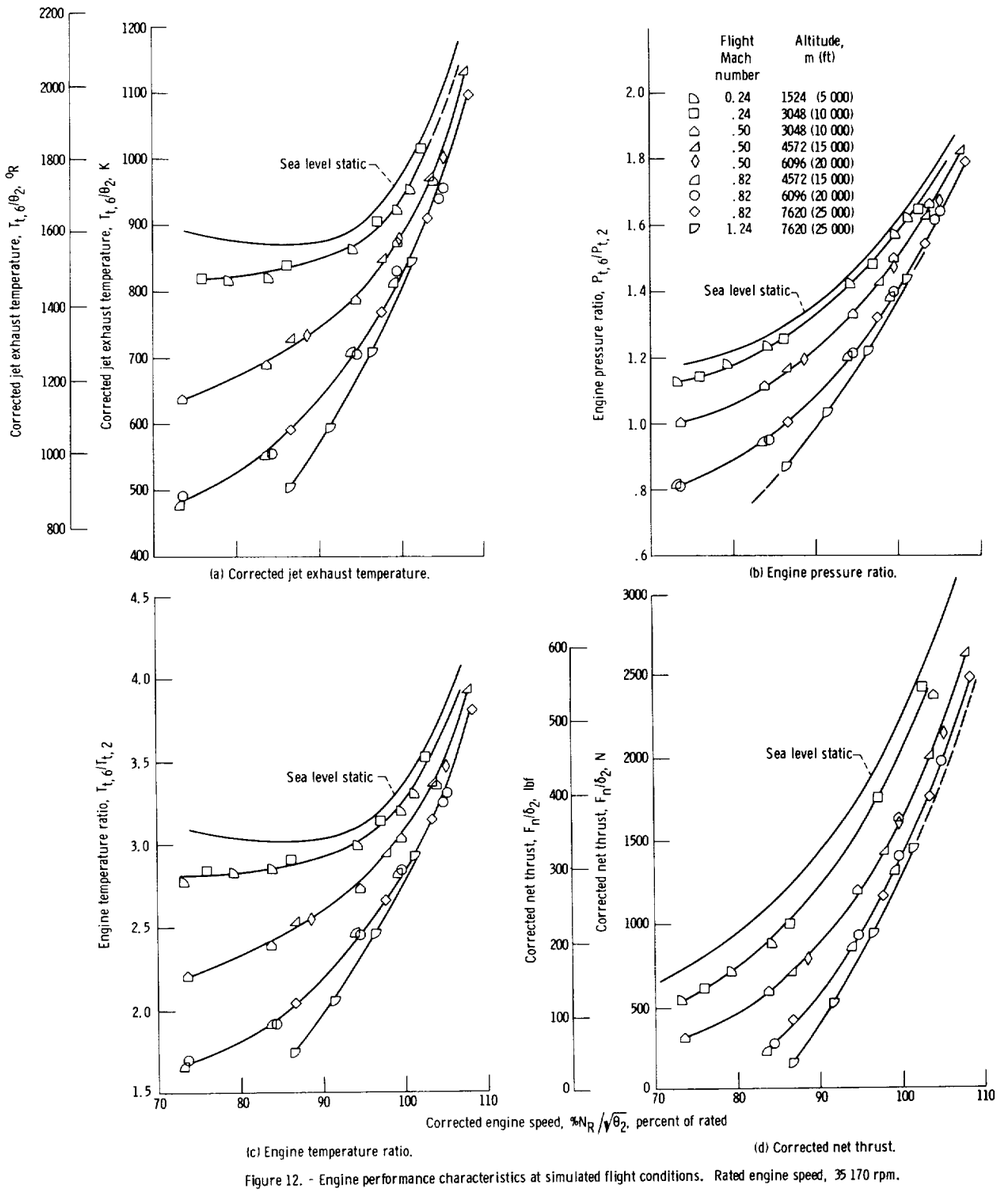
Figure 12. - Engine performance characteristics at simulated flight conditions. Rated engine speed, 35 170 rpm.

26

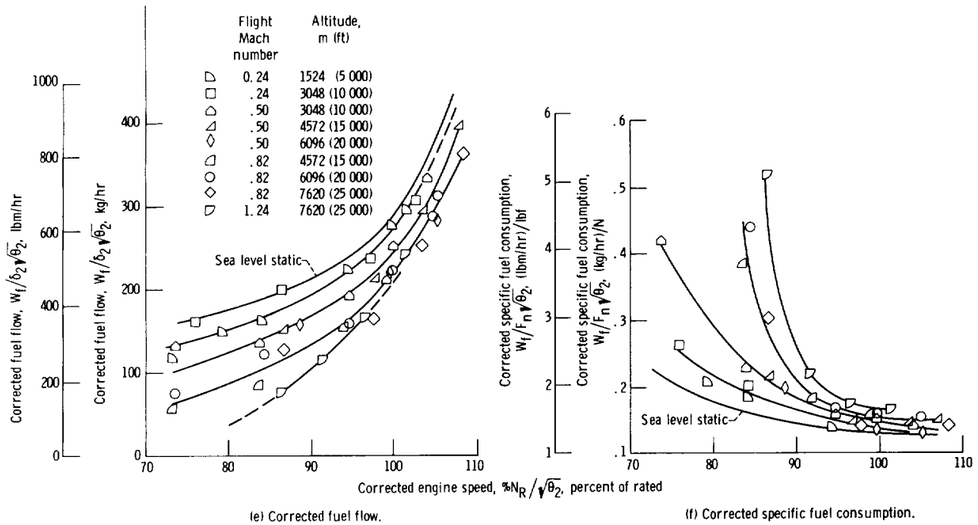

(e) Corrected fuel flow.

(f) Corrected specific fuel consumption.

Figure 12. - Concluded.

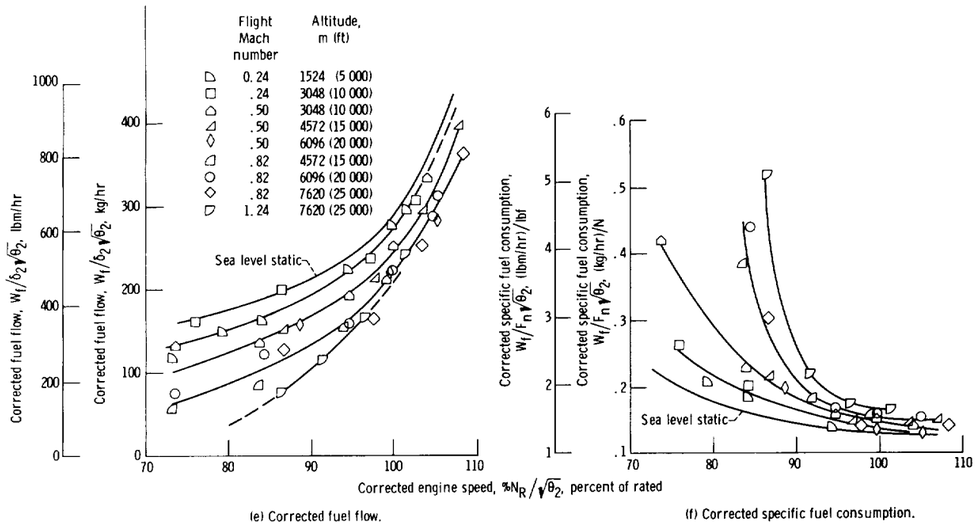

(e) Corrected fuel flow.

(f) Corrected specific fuel consumption.

Figure 12. - Concluded.

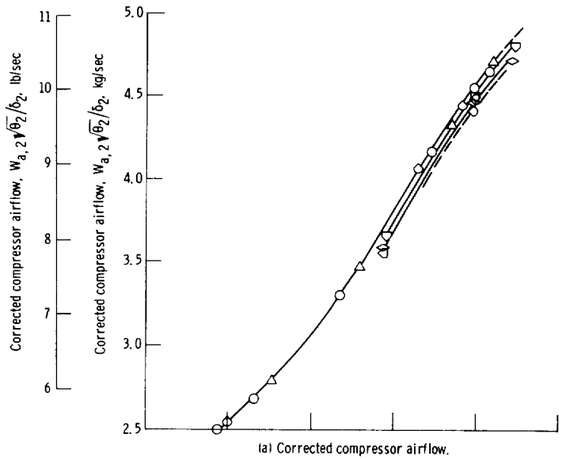

(a) Corrected compressor airflow.

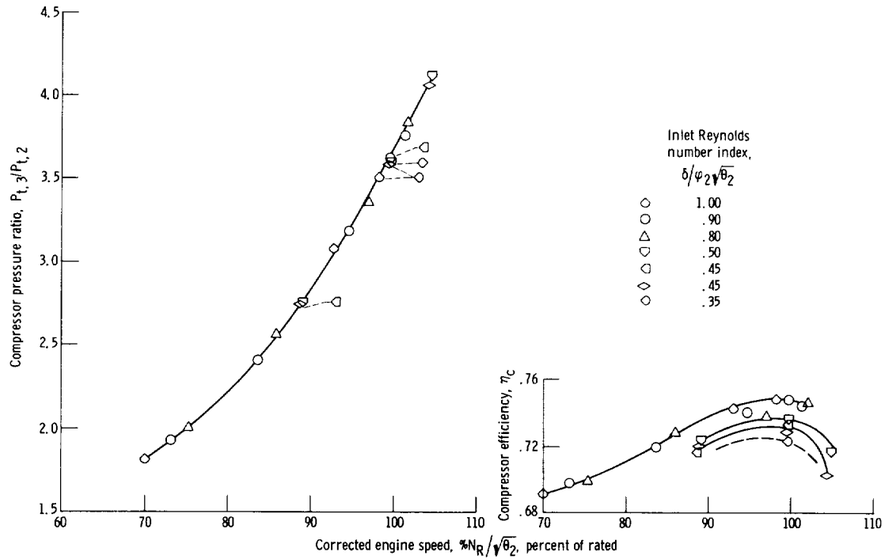

(b) Compressor pressure ratio.

(c) Compressor efficiency.

Figure 13. - Compressor characteristics for nominal flight Mach number of 0.38. Rated engine speed, 35 170 rpm.

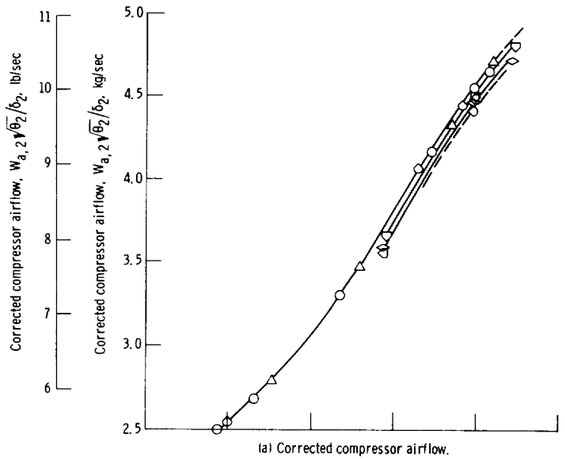

(a) Corrected compressor airflow.

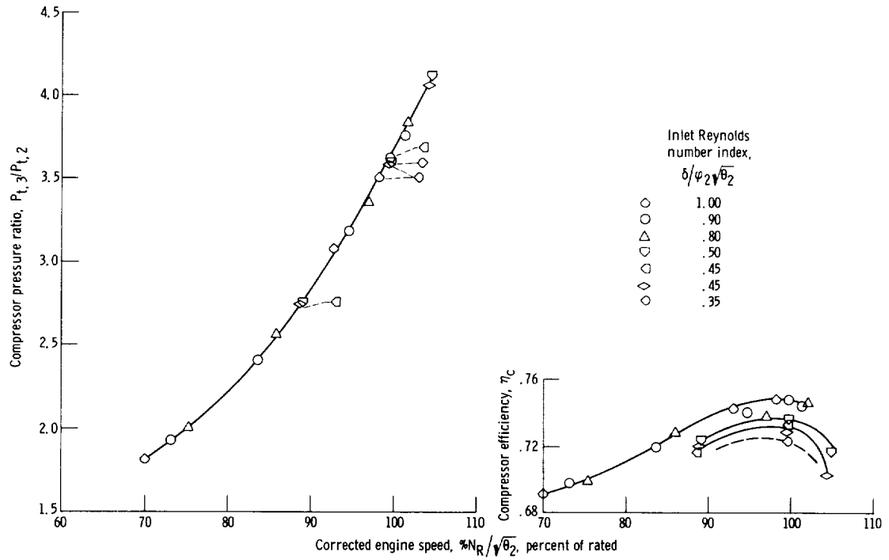

(b) Compressor pressure ratio.

(c) Compressor efficiency.

Figure 13. - Compressor characteristics for nominal flight Mach number of 0.38. Rated engine speed, 35 170 rpm.

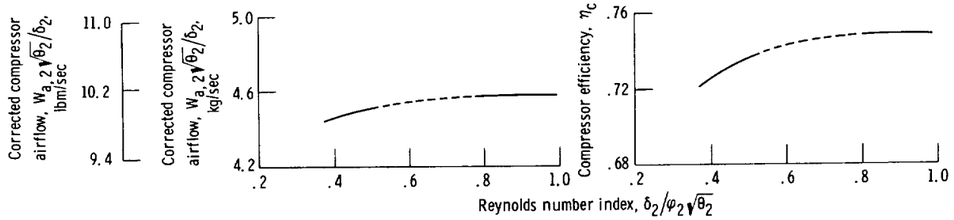

(a) Corrected compressor airflow. (b) Compressor efficiency.

Figure 14. - Compressor characteristics as function of inlet Reynolds number index ($M_0 \approx 0.38$; $\%N_R/\sqrt{\theta_2} = 100$). Rated engine speed, 35 170 rpm.

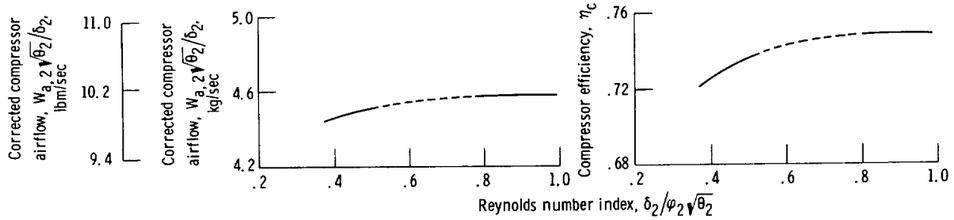

(a) Corrected compressor airflow. (b) Compressor efficiency.

Figure 14. - Compressor characteristics as function of inlet Reynolds number index ($M_0 \approx 0.38$; $\%N_R/\sqrt{\theta_2} = 100$). Rated engine speed, 35 170 rpm.

NASA-Langley, 1976 E-8775 29